

AD-A197 438

DTIC FILE COPY

4

MEMORANDUM REPORT BRL-MR-3674

**BRL**

1938 - Serving the Army for Fifty Years - 1988

INTERNAL PRESSURE MEASUREMENTS FOR A  
LIQUID PAYLOAD AT LOW REYNOLDS NUMBERS

DAVID J. HEPNER  
KEITH P. SOENCKSEN  
BRADFORD S. DAVIS  
NICHOLAS G. MAIORANA

JUNE 1988

DTIC  
SELECTED  
JUL 08 1988  
S E D

APPROVED FOR PUBLIC RELEASE; DISTRIBUTION UNLIMITED.

U.S. ARMY LABORATORY COMMAND

**BALLISTIC RESEARCH LABORATORY**  
**ABERDEEN PROVING GROUND, MARYLAND**

DESTRUCTION NOTICE

Destroy this report when it is no longer needed. DO NOT return it to the originator.

Additional copies of this report may be obtained from the National Technical Information Service, U.S. Department of Commerce, Springfield, VA 22161.

The findings of this report are not to be construed as an official Department of the Army position, unless so designated by other authorized documents.

The use of trade names or manufacturers' names in this report does not constitute indorsement of any commercial product.

UNCLASSIFIED

SECURITY CLASSIFICATION OF THIS PAGE

REPORT DOCUMENTATION PAGE				Form Approved OMB No 0704-0188 Exp Date Jun 30, 1986		
1a REPORT SECURITY CLASSIFICATION UNCLASSIFIED			1b. RESTRICTIVE MARKINGS			
2a SECURITY CLASSIFICATION AUTHORITY			3. DISTRIBUTION / AVAILABILITY OF REPORT Approved for public release; distribution is unlimited			
2b DECLASSIFICATION / DOWNGRADING SCHEDULE						
4. PERFORMING ORGANIZATION REPORT NUMBER(S) BRL-MR-3674			5. MONITORING ORGANIZATION REPORT NUMBER(S)			
6a NAME OF PERFORMING ORGANIZATION U.S. Army Ballistic Research Laboratory		6b. OFFICE SYMBOL (If applicable) SLCBR-LF		7a. NAME OF MONITORING ORGANIZATION		
6c. ADDRESS (City, State, and ZIP Code) Aberdeen Proving Ground, MD 21005-5066			7b. ADDRESS (City, State, and ZIP Code)			
8a. NAME OF FUNDING / SPONSORING ORGANIZATION U.S. Army Ballistic Research Laboratory		8b OFFICE SYMBOL (If applicable) SLCBR-DD-T		9. PROCUREMENT INSTRUMENT IDENTIFICATION NUMBER		
8c. ADDRESS (City, State, and ZIP Code) Aberdeen Proving Ground, MD 21005-5066			10. SOURCE OF FUNDING NUMBERS			
			PROGRAM ELEMENT NO. 62618A	PROJECT NO 1L1 62618AH80	TASK NO	WORK UNIT ACCESSION NO
11 TITLE (Include Security Classification) (Unclassified) INTERNAL PRESSURE MEASUREMENTS FOR A LIQUID PAYLOAD AT LOW REYNOLDS NUMBERS						
12 PERSONAL AUTHOR(S) Hepner, David J., Soencksen, Keith P., Davis, Bradford S., Maiorana, Nicholas G.						
13a TYPE OF REPORT Memorandum Report		13b TIME COVERED FROM _____ TO _____		14. DATE OF REPORT (Year, Month, Day) 1988 April		
15. PAGE COUNT 57						
16. SUPPLEMENTARY NOTATION						
17			18. SUBJECT TERMS (Continue on reverse if necessary and identify by block number)			
COSATI CODES			Internal Liquid Pressure Measurements Scaled Simulations of Viscous Payloads			
FIELD	GROUP	SUB-GROUP				
01	01					
19	06					
19. ABSTRACT (Continue on reverse if necessary and identify by block number) (jvs/bja)  Scaled simulations of high viscosity liquid payloads were completed for a Reynolds number range of 3.1 - 8.9. Testing included establishing instrumentation reliability, repeating previously published low Reynolds number data, expanding the range in nondimensional coning frequency and Reynolds number, and providing a data base for comparisons with current linear theory applications at low Reynolds number. Based on these preliminary results, extensive testing can be accomplished on the BRL Flight Simulator using a full-scale cylinder and larger instrumentation payload capacity.						
20 DISTRIBUTION / AVAILABILITY OF ABSTRACT <input type="checkbox"/> UNCLASSIFIED/UNLIMITED <input checked="" type="checkbox"/> SAME AS RPT <input type="checkbox"/> DTIC USERS			21 ABSTRACT SECURITY CLASSIFICATION UNCLASSIFIED			
22a NAME OF RESPONSIBLE INDIVIDUAL David J. Hepner			22b TELEPHONE (Include Area Code) (301)-278-2533		22c OFFICE SYMBOL SLCBR-LF-A	

# ACKNOWLEDGMENTS

The authors greatly appreciate the contribution of the following individuals. Mr. Lawrence Burke for technical support, Mr. Tom Kendall and Mr. A. Macintosh for graphics, and Ms Joyce Smith for report preparation.

Accession For		
NTIS	OWI	<input checked="" type="checkbox"/>
ERIC	OWI	<input type="checkbox"/>
Unannounced		<input type="checkbox"/>
Justification		
By		
Dissemination		
Availability Codes		
Available and/or		
Dist	Special	
A-1		



## TABLE OF CONTENTS

	<u>Page</u>
ACKNOWLEDGMENTS.....	iii
LIST OF FIGURES.....	vii
LIST OF TABLES.....	viii
I. INTRODUCTION.....	1
II. EXPERIMENT DESCRIPTION AND OBSERVATIONS.....	2
III. DATA REDUCTION.....	4
IV. CONCLUSIONS.....	7
LIST OF REFERENCES.....	51
LIST OF SYMBOLS.....	53
DISTRIBUTION LIST.....	55

# LIST OF FIGURES

Figure		Page
1	Cubic spline fit to experimental data for various high Reynolds number cases (Ref. 2).....	8
2	Cylinder dimensions and transducer locations.....	9
3	Forced precession gyroscope apparatus.....	10
4	Precession angle adjustment cam.....	11
5	Pressure gage calibration for $r/a = 0.667$ .....	12
6	Instrumentation schematic.....	13
7	High pass filter amplifier transfer function.....	14
8	Liquid viscosity measurements and logarithmic function fit.....	15
9	Absolute pressure decrease on an end wall for a slow spin-up....	16
10	Absolute pressure rise for extended running time, (coning rate = 5 Hz, spin rate = 70 Hz).....	17
11	Spectral response for oscillatory pressures.....	18
12	Spectra of several runs overlayed for low Reynolds number.....	19
13	Prograde pressure coefficient data for two radial positions ( $r/a = 0.434$ and $0.667$ at $Re$ near 8.8, $\alpha = 2.25^\circ$ ).....	20
14	Prograde and retrograde pressure coefficient comparison with modified Ref. 3 data for $Re$ near 8.8, $\alpha = 2.00^\circ$ , $r/a = 0.667$ ..	21
15	Experimental prograde data ( $f = .92$ ), $\Delta = 0.022^\circ$ , $\square = 0.051^\circ$ , $x = 0.105^\circ$ , $\diamond = 0.22^\circ$ , $\circ = 0.50^\circ$ (Ref. 2).....	22
16	Prograde and retrograde pressure coefficient comparison for linearity with coning angle, $Re = 7.3$ , $\alpha = 0.5, 1$ and $2$ deg, $r/a = 0.667$ .....	23
17	Expanded coning frequency and error ranges due to low spin rates	24
18	Prograde and retrograde pressure coefficient data for $Re = 5.2$ , $\alpha = 2.00^\circ$ , $r/a = 0.667$ .....	25
19	Prograde and retrograde pressure coefficient data for $Re = 3.1$ , $\alpha = 2.00^\circ$ , $r/a = 0.667$ .....	26
20	Comparison of experimental data to two available low Reynolds number theories for $Re = 3.1$ .....	27

# LIST OF FIGURES (continued)

<u>Figure</u>		<u>Page</u>
21	Comparison of experimental data to two available low Reynolds number theories for $Re = 8.7$ .....	28

## LIST OF TABLES

<u>Table</u>		<u>Page</u>
1	Cavity Dimensions of Lucite Cylinder with Various Inserts.....	29
2	Reynolds Number Calculations for Available Spin Rates and Actual Liquid Viscosities for an Internal Cylinder Radius of 3.176 cm	30
3	Absolute Pressure Measurements and Predicted Pressure Differences for Constant Spin Rates.....	31
4	Absolute Pressure Measurements for Constant Spin (70 Hz) and Coning Motion (5 Hz).....	32
5	Forced Precession Gyroscope System Errors.....	33
6a	Prograde Oscillatory Pressure Data for $Re = 8.7$ , $\alpha = 2.25^\circ$ , $r/a = 0.667$ .....	34
6b	Prograde Oscillatory Pressure Data for $Re = 8.7$ , $\alpha = 2.25^\circ$ , $r/a = 0.434$ .....	35
7a	Prograde Oscillatory Pressure Data for $Re = 8.7$ , $\alpha = 2.00^\circ$ , $r/a = 0.667$ .....	36
7b	Retrograde Oscillatory Pressure Data for $Re = 8.7$ , $\alpha = 2.00^\circ$ , $r/a = 0.667$ .....	37
8a	Prograde Oscillatory Pressure Data for $Re = 7.3$ , $\alpha = 0.50^\circ$ , $r/a = 0.667$ .....	38
8b	Retrograde Oscillatory Pressure Data for $Re = 7.3$ , $\alpha = 0.50^\circ$ , $r/a = 0.667$ .....	39
9a	Prograde Oscillatory Pressure Data for $Re = 7.3$ , $\alpha = 1.00^\circ$ , $r/a = 0.667$ .....	40
9b	Retrograde Oscillatory Pressure Data for $Re = 7.3$ , $\alpha = 1.00^\circ$ , $r/a = 0.667$ .....	41
10a	Prograde Oscillatory Pressure Data for $Re = 7.3$ , $\alpha = 2.00^\circ$ , $r/a = 0.667$ .....	42

# LIST OF TABLES (continued)

<u>Table</u>		<u>Page</u>
10b	Retrograde Oscillatory Pressure Data for $Re = 7.3$ , $\alpha = 2.00^\circ$ , $r/a = 0.667$ .....	43
11a	Prograde Oscillatory Pressure Data for $Re = 5.2$ , $\alpha = 2.00^\circ$ , $r/a = 0.667$ .....	44
11b	Retrograde Oscillatory Pressure Data for $Re = 5.2$ , $\alpha = 2.00^\circ$ , $r/a = 0.667$ .....	45
12a	Prograde Oscillatory Pressure Data for $Re = 3.1$ , $\alpha = 2.00^\circ$ , $r/a = 0.667$ .....	46
12b	Retrograde Oscillatory Pressure Data for $Re = 3.1$ , $\alpha = 2.00^\circ$ , $r/a = 0.667$ .....	47
13	Comparison of Experimental Data to Two Available Low Reynolds Number Theories for $Re = 3.1$ .....	48
14	Comparison of Experimental Data to Two Available Low Reynolds Number Theories for $Re = 8.7$ .....	49



## I. INTRODUCTION

Spin-stabilized projectiles can experience poor flights due to the influence of liquid payloads. Substantial analytical and numerical work has been done on this problem, but quality experimental data on the primitive variables of the liquid (pressure and velocity) are still required to evaluate the accuracy and applicability of models and codes.

Scaled laboratory experiments simulating spin-stabilized, liquid-filled cylinders and comparisons with theory have been reviewed by Sedney.<sup>1</sup> The history of experimental pressure measurements at the US Army Ballistic Research Laboratory (BRL), Aberdeen Proving Ground, Maryland has included many scaled simulations in a small, forced precession gyroscope fixture. Whiting reported liquid pressure measurements for a range of relatively high Reynolds numbers (5,000 to 500,000).<sup>2</sup> For high Reynolds number cases, Whiting found that the liquid behaves in a resonant manner where a maximum pressure coefficient was found by varying the ratio of coning to spin frequencies ( $\tau$ ). Measured and computed pressures were compared for very small angles of attack (typically less than 1 degree). Figure 1 represents a cubic spline fit to experimental data from Reference 2. Nonlinear and aperiodic pressures were also observed, but few general conclusions were made. Using the same techniques, a single series of measurements were completed by Nusca, Beims, and D'Amico for a Reynolds number of 8.8.<sup>3</sup> They found pressure responses to be almost linear with  $\tau$ . Experimentally, the linearity with coning frequency at lower Reynolds numbers may be a result of the resonance curve broadening and flattening with increased viscous forces. Hence, for very low Reynolds numbers the linear results tend to occur over a small range of a resonance curve. Cone-up pressure data were documented for a single cylinder aspect ratio, geometry and Reynolds number.<sup>4</sup> Other laboratory experiments simulating spin-stabilized, liquid-filled projectiles have been performed by D'Amico<sup>5</sup> to examine liquid coning for low Reynolds numbers. In D'Amico's experiments with Reynolds numbers greater than 1,000, the transverse moment of inertia of a free gyroscope was varied to find the frequency of motion where maximum coning growth would occur, i.e., a resonance peak. In free gyroscope tests for Reynolds numbers less than 100, the broadening effect of low Reynolds numbers is also evident. Evidence of related liquid instabilities for actual flight data was reported in References 6-8. Recently, a full-scale three-degree-of-freedom flight simulator was used to examine both endwall and sidewall pressure fluctuations, as well as the phase relationship between the maximum pressure and cylinder orientation for a high Reynolds number of 18,200.<sup>9-10</sup>

Typically, pressure responses are resonant in nature for Reynolds numbers above 1,000. The periodic part of the pressure can lead to destabilizing moments that are controlled by a particular set of physical parameters: cylinder aspect ratio ( $c/a$ ), Reynolds number ( $Re$ ), coning angle ( $\alpha$ ), and coning frequency ( $\tau$ ). The aspect ratio is defined as the ratio of cylinder height to diameter. The Reynolds number is defined as the product of spin rate (rad/sec) and radius squared divided by the liquid kinematic viscosity. Finally,  $\tau$  is defined as the ratio of coning frequency to the inertial spin frequency.

It was noted in Reference 3 that higher values of  $\tau$  would be difficult to achieve for spin rates of 83.3 Hz. It was thought that an extended range for  $\tau$  would eventually show a resonance similar to the high Reynolds number

condition.

Recently, increases in the range of Reynolds number and  $\tau$  were made possible by using low spin rates. In this series of experiments, a large range of  $\tau$  was achieved by reduction of the spin rate, yielding a maximum  $\tau$  of 0.383 (a coning rate of 11.5 Hz and a spin rate of 30 Hz). Improvements in equipment reliability have led to more repeatable oscillatory pressure measurements and have allowed measurements of internal absolute pressures. On-board circuits and a twelve-channel slip ring have replaced the previous instrumentation/telemetry system (which consisted of on-board batteries, amplification and a transmitter/antenna). In this new series of tests, power to the associated circuits and transducers was passed to the rotating frame via the slip ring; hence, long run times were possible since batteries were not used (as in References 2, 3 and 5). Optical speed sensors have replaced inductive pickups to measure spin and coning frequencies.

## II. EXPERIMENT DESCRIPTION AND OBSERVATIONS

The forced precession apparatus is documented in References 2 and 3 and has remained relatively unchanged. Sketches showing the cylinder, gyroscope, and coning drive are reproduced (with slight modifications where applicable) in Figures 2-4. The same cylinder and endcaps are used for these experiments. Other inserts are available and the resulting dimensions are given in TABLE 1. The lucite cylinder was refitted with drive spindles which place the geometric center of the cavity at the gimbal axis to within .01". The top cylinder endcap was fitted with two semiconductor pressure gages at positions  $r/a = 0.434$  and  $0.667$ . Pressure gage calibrations were completed and a sample is shown in Figure 5. The two channel amplifier/filter circuit was designed and constructed to fit in the same endcap (Figure 6). A typical transfer function for the two channel circuit is shown in Figure 7. A hollow support tube allowed ribbon wire access to the slip ring assembly. The twelve-channel slip ring was mounted to the cage and rotated with the rotor assembly at the spin frequency. The slip ring allowed the transfer of power and pressure signals with approximately 0.24mV RMS noise amplitude at the spin frequency. Power channels were low-pass filtered to eliminate spin noise and stray 60 Hz. Two low voltage oscillatory signals and two low level differential DC signals were transferred from the rotating frame to the laboratory frame (Figure 6). Circuit power supply lines which provided  $\pm 10.0$  volts and a ground reference to the rotating frame are not shown for clarity.

Silicon oil with a nominal kinematic viscosity of 60,000 centistokes (cs) was used to fill the cavity. One centistoke is defined as:  $1 \text{ cs} = 1 \text{ cm}^2/\text{sec} \approx$  kinematic viscosity of water at standard conditions. The silicon oil viscosity and densities were measured for four temperatures:

<u>Temp (°C)</u>	<u>Density (g/ml)</u>	<u>Viscosity (cs)</u>
20.0	0.973	67,100
25.0	0.969	60,600
30.0	0.965	54,800
35.0	0.961	50,100

For the 15 degree temperature range, the density varied 1.2% and the viscosity differed 25% using the 20 degree measurements as a reference. The viscosity data were fitted using a base 10 logarithmic function (Figure 8). The cylinder was evacuated after filling to remove absorbed air. The cylinder was then sealed (at 100% fill and at 25°C). This temperature was chosen as optimum for testing purposes since it is close to normal room temperatures. The thermal expansion coefficients of the lucite cylinder, aluminum endcaps, and silicon oil are considerably different and even small room temperature changes can produce voids or overpressures in the cavity. Other oil viscosities are available in nominal values ranging from 1 to 100,000 cs. Given the constant cavity radius ( $a = 3.1761$  cm), a set of Reynolds number ranges for various spin rates are shown in TABLE 2.

After assembly was complete, the entire rotor was dynamically balanced and placed into the cage assembly. The cage permitted precession angles (coning angle) from .5 to 3 degrees. The coning angle was calculated by measuring run-out with a dial indicator set near the cam surface. The angle is simply the arc tangent of the run-out divided by the vertical displacement of the indicator from the gimbal axes. An adjustable cam and bushing assembly holds the cage firmly in position. The coning angle is variable from 2.5 to 12 Hz. The spin drive is a DC motor capable of spin frequencies from 30 to 83.3 Hz. Varying the spin was the easiest method for producing small changes in Reynolds number.

Slow, steady spin-ups of a 100% filled cylinder produced variations in internal absolute pressures. A general decrease in absolute pressure with increasing spin was observed (TABLE 3 and Figure 9). The run time was relatively short (3 min) for the case where the spin frequency was varied from 0-80 Hz without coning motion. It was observed that the inner gage always responded with a lower absolute pressure than the outer gage. Spinning reduced the internal cylinder pressure on the endwall at these two radial positions. The absolute pressure difference between gages for any spin rate is given by:

$$\Delta P = \frac{\rho}{2} (r_2^2 - r_1^2) \omega^2$$

A comparison between predicted pressure difference and experimental difference is also in TABLE 3. Absolute pressures were monitored continuously to remain within the gage linear response region.

The oscillatory responses of the gages were recorded, reduced, and compared with previous data. All data runs within one test set (as many as 19 runs) are for a single, constant spin rate and take approximately 20 to 30 minutes to complete. The entire system was allowed sufficient time to reach steady-state for each coning frequency according to a settling time based on the inherent viscous processes for low Reynolds numbers:

$$\text{Settling Time (sec)} = \text{Re} / \text{Spin (rad/sec)}. \quad (1)$$

While the cylinder was spinning and coning, the internal absolute pressure would rise steadily due to viscous heating. After an extensive running

time, this heating caused the fluid to expand and pressurize (and eventually overpressurize) the gages beyond the 50 psia linear limit. The gages were not damaged since internal mechanical stops protect against overpressures to 1000 psia. No oscillating pressure signals were measured above 50 psia, and the system was allowed to cool overnight. If the room temperature was below 24°C, a vacuum bubble was observed within the cavity. Experimental runs were only started after room temperature increased so as to eliminate the vacuum bubble. (Future testing will include a temperature measurement system using thermistors to accurately monitor liquid temperatures.)

The absolute pressures measured over an extended period of time are listed in TABLE 4 and illustrated by Figure 10. The resulting history of oscillatory pressure signals remained unchanged while within the linear gage region. The internal pressure increase and the liquid temperature increase produced no change in oscillatory amplitudes. The oscillatory pressure spectra are not sensitive to small variations in liquid viscosity, density or internal cavity pressure. The liquid temperature increase over the course of this test was measured after the cylinder was quickly disassembled. The overpressure condition corresponded to a liquid temperature of 26.9°C. The change in viscosity and density with temperature, as found by fitting data, was 3.4% in viscosity and 0.16% in density. Since internal temperature was not actually monitored, experimental errors were assumed to be  $\pm 1\%$  for density and  $\pm 4\%$  for viscosity. All calculations involving viscosity and density use the 25° measured values.

### III. DATA REDUCTION

A typical oscillatory pressure record includes responses for at least two frequencies: one is a function of the forced oscillation produced by the coning motion, while a second, and normally smaller response, occurs at the spin frequency (Figure 11). The response at the spin frequency is a residual effect resulting from a small dynamic imbalance in the system. Varying the coning rate and overlaying several spectra produces an overlay map (Figure 12). A pressure coefficient ( $\hat{C}_p$ ) can be defined using the Fourier amplitude of the oscillating pressure and appropriate scale factors,

$$\hat{C}_p = \frac{\hat{P}\hat{\gamma}}{\alpha \rho a^2 p^2} \quad (2)$$

where  $\hat{P}$  is the oscillating pressure peak amplitude

$\alpha$  is the precession angle

$\rho$  is the fluid density

$a$  is the cylinder radius

$p$  is the cylinder inertial spin rate

$\hat{\gamma}$  is  $\frac{\tau}{|\tau|}$

Prograde precession is established when both the precession and spin vectors rotate in the same direction. Retrograde precession is defined when spin and coning have opposite senses of rotation. Response plots show the pressure coefficient versus  $\tau$ .  $\hat{C}_p$  and  $\tau$  are sensitive to the relative rotation sense of the spin and precession. Hence,  $\hat{C}_p$  and  $\tau$  are positive for prograde motion and both negative for retrograde motion. A tabulation of all oscillating pressure measurements and coefficient calculations are given for each set of experiments.

Prior to the first data runs, gyroscope system errors based on instrument and apparatus capabilities were determined. These are listed in TABLE 5. The plotted data include error bars as a measure of the total system error. The maximum and minimum  $\hat{C}_p$  values are calculated from the error parameters. For example, maximum values are simply the result of calculating  $\hat{C}_p$  with the largest pressure (pressure plus pressure error) divided by the smallest scale factors (factor minus factor error). Error calculations in pressure coefficients are tabulated as minimum and maximum values. These values are shown as the vertical range of error bars.  $\tau$  errors are represented by the horizontal span of error caps. Error bars are omitted on some graphs for clarity.

The first experiments were performed at a Reynolds number of 8.7. The coning angle was set at 40 mils ( $2.25^\circ$ ) using a gunner's quadrant. This method proved ineffective for smaller angles with a measurement error of 0.5 mil. Thus, smaller angles were set using a dial indicator. The data were taken for prograde motion at 10 intervals of increasing coning rate. Additional measurements were taken as the coning speed was reduced to the slowest rate. The results are tabulated in TABLES 6a and 6b.  $\hat{C}_p$  values for the two transducer positions are plotted in Figure 13. Throughout all of the tests,  $\hat{C}_p$  values for  $r/a = 0.667$  always produced larger pressure coefficient values than  $r/a = 0.434$ . This test verified the preliminary findings of Reference 3 where pressure varied nearly linearly with increasing nondimensional coning frequency ( $\tau$ ).

A minor modification to Reference 3 data included more exact density and viscosity measurements extracted from Reference 6. One more test was performed at this Reynolds number of 8.7. Sets of data are included as TABLES 9a and 9b. The data were taken for prograde and retrograde motion transducer position = 0.667. A plot of both prograde and retrograde data (TABLES 7a and 7b) with modified Reference 3 data depicts the small differences between the data (Figure 14). Differences in gyroscope apparatus, liquids used, and data collection account for the data discrepancies. The new data encompass nearly all the Reference 3 data within the  $\hat{C}_p$  error range. Considering the change in apparatus (see References 2 and 3), it can be stated that the replication of previous results has been accomplished.

The next area of experimentation was the verification of linear theory applications (linear with coning angle) for low Reynolds numbers. At sufficiently large coning angles and for high Reynolds number, the pressure

coefficient data showed nonlinear (not linear in coning angle) and even aperiodic responses for prograde motion.<sup>2</sup> Figure 15 is reproduced from Reference 2. For a Reynolds number of 80,000, the nonlinearities first occur at a coning angle of 0.22 degrees. Vertical lines connecting two points represent the aperiodic fluctuations in pressure. They are not representative of system errors. Figure 15 data also shows frequency shifts for the nonlinear data. For lower Reynolds numbers (as low as 10,000), Whiting found the nonlinearities to occur at a higher coning angle.<sup>2</sup>

A set of experiments were conducted at the coning angles of 0.5, 1 and 2. The coning cam bushing was replaced by a thin set of roller bearings and the coning angle was limited to a maximum of two degrees. Future testing will include a new cam design using roller bearings. The spin rate was lowered to 70.0 Hz to extend roll bearing life. The experiments were run in much the same fashion as previous tests. Nineteen runs were completed at each angle for both prograde and retrograde motions and both transducer positions. The final data are tabulated for coning angle = 0.5 degrees in TABLES 8a-b. Likewise, data for a coning angle of 1.0 degree are listed in TABLES 9a-b. TABLES 10a-b are arranged similarly for a coning angle of 2.0 degrees.  $Re = 7.3$  data are plotted in Figure 16 where prograde and retrograde are shown for the radial position = 0.667. The 0.5 degree data differ considerably due to the small coning angle and low signal levels. When viewed on this scale the data do not show the nonlinear trends evidenced by Whiting at higher Reynolds numbers.

Another aim of the experimental work was to investigate extending the range of  $\tau$  by simply decreasing the spin rate. For the same range in coning rates, an extended range of  $\tau$  results. A change in spin also affects a change in Reynolds number. Reynolds number 3.1 is the result of a spin rate of 30 Hz and a  $\tau$  ranging from -0.383 to 0.383. The Reynolds number 8.7 is attained at a spin rate of 83.3 Hz and  $\tau$  ranges from -0.138 to 0.138. The relative extension in  $\tau$  for lower spin rates is evident from a comparison of Reynolds number 3.1 - 8.7 is shown in Figure 17. Larger errors in amplifier gain occur due to the high pass filtering characteristics and low spin rates. Several tests were run at medium spin rates of 50.0 Hz and 30 Hz. Measurements were taken for prograde and retrograde motions for  $r/a = 0.667$ . TABLES 11a and 11b list data for Reynolds number 5.2 (Figure 18). TABLES 12a and 12b give data for Reynolds number 3.1 (Figure 19). The experimental  $\hat{C}_p$  data for Reynolds number 3.1 seem to have a nonlinear dependence upon  $\tau$ , resembling the leading edge of a resonant response curve.

An example of two theories which are applicable at low Reynolds number are the spatial eigenvalue method and the University of Wisconsin's finite difference method. These codes are available at BRL.

The spatial eigenvalue method developed by Hall, Sedney and Gerber<sup>11</sup> reduces the incompressible Navier-Stokes equations to a set of linear partial differential equations. The angle of coning motion is assumed small. A particular solution is employed that satisfies the axial and lateral cylinder wall boundary conditions. The flow variables are expressed as eigenfunction expansions with the coefficients determined by satisfying the cylinder endwall boundary conditions; a least squares method has been used for this purpose. The method runs very efficiently (less than 10 cpu seconds) on a VAX 8600

mini-computer for low Reynolds numbers ( $< 100$ ) with small increases in computer run time for larger Reynolds number values up to 2000.

University of Wisconsin's computation solves the steady state, incompressible Navier-Stokes equations, including non-linear effects, for a precessing/spinning cylinder at a fixed precession angle. The code uses an iterative finite-difference method based on modified line successive-over-relaxation and a pressure update from the gradient of the velocity field. Nusca<sup>12</sup> has shown that the code runs efficiently: (less than 1 cpu hour) on a VAX 8600 mini-computer for low Reynolds numbers ( $< 80$ ) but requires the use of a CRAY XMP computer for larger Reynolds number values up to 300.

Comparisons of experiment to the two theories are given in Figures 20 and 21 and TABLES 13 and 14. These theories aid in examining trends and extrapolation past experiment capabilities.

#### IV. CONCLUSIONS

A small gyroscope fixture was used to carry a liquid-filled cylinder at relatively low spin and coning rates. The experiments were conducted under controlled, repeatable conditions. The purpose of the experiments was to provide a basis for full-scale simulations of liquid payloads. Based on these preliminary results, extensive testing can be accomplished on the BRL Flight Simulator using a full-scale cylinder and larger instrumentation payload capacity.

Oscillatory and absolute pressure data were obtained for a relatively low Reynolds number range. Testing included establishing instrumentation reliability, repeating previously published low Reynolds number data, expanding the range in nondimensional coning frequency and Reynolds number, and providing a data base for comparisons with current linear theory applications at low Reynolds number.

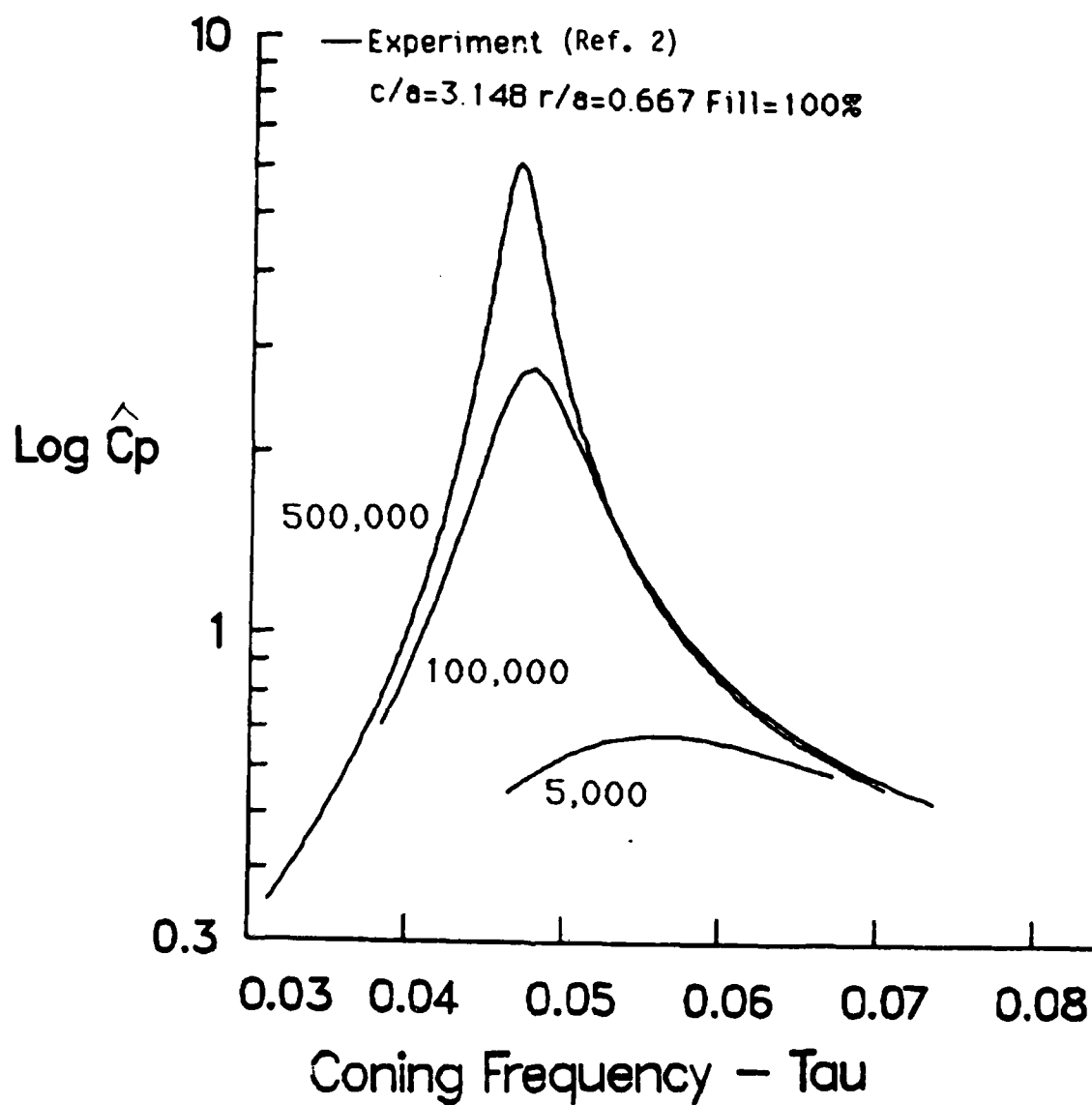


Figure 1. Cubic spline fit to experimental data for various high Reynolds number cases (Ref. 2).



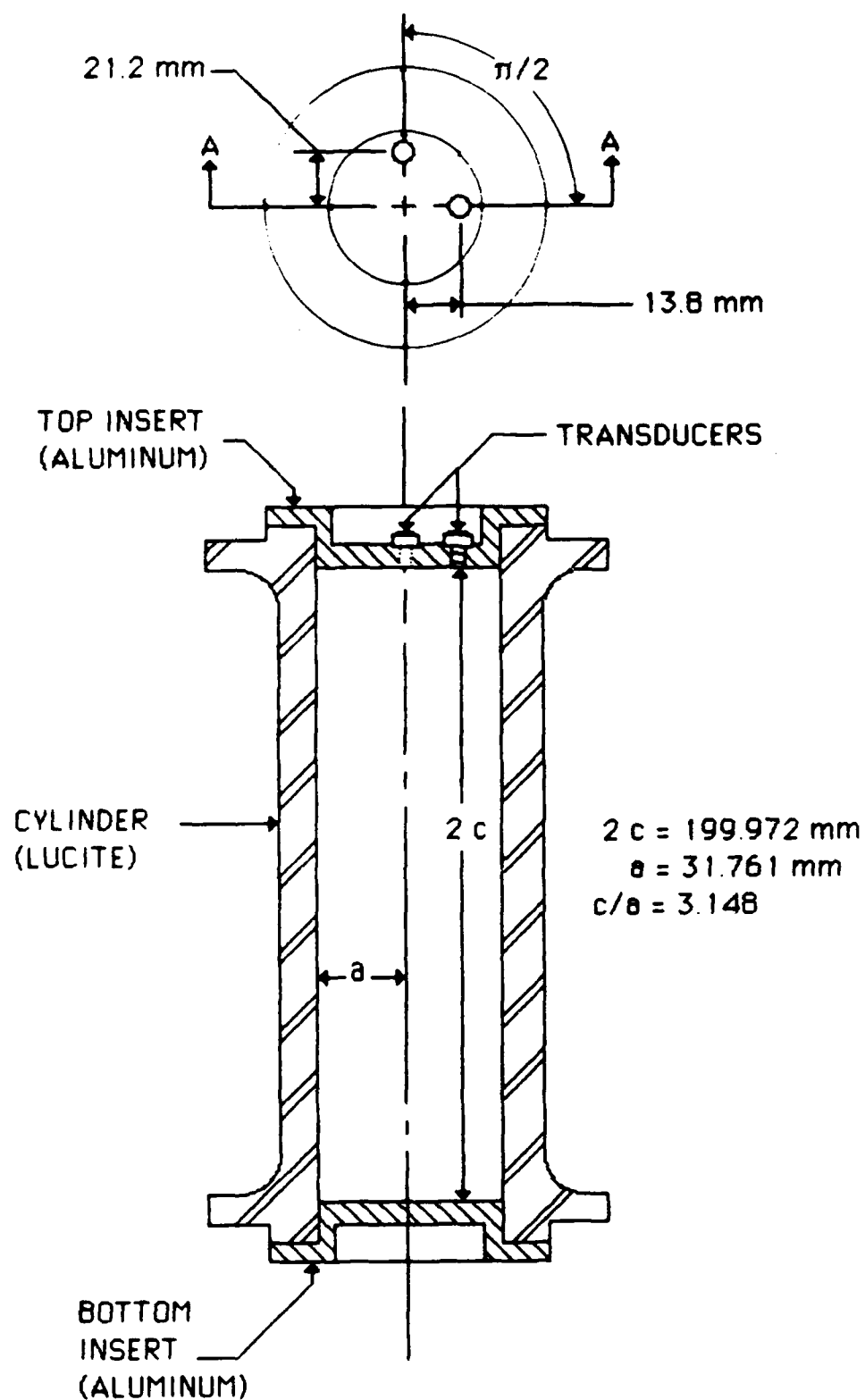


Figure 2. Cylinder dimensions and transducer locations.

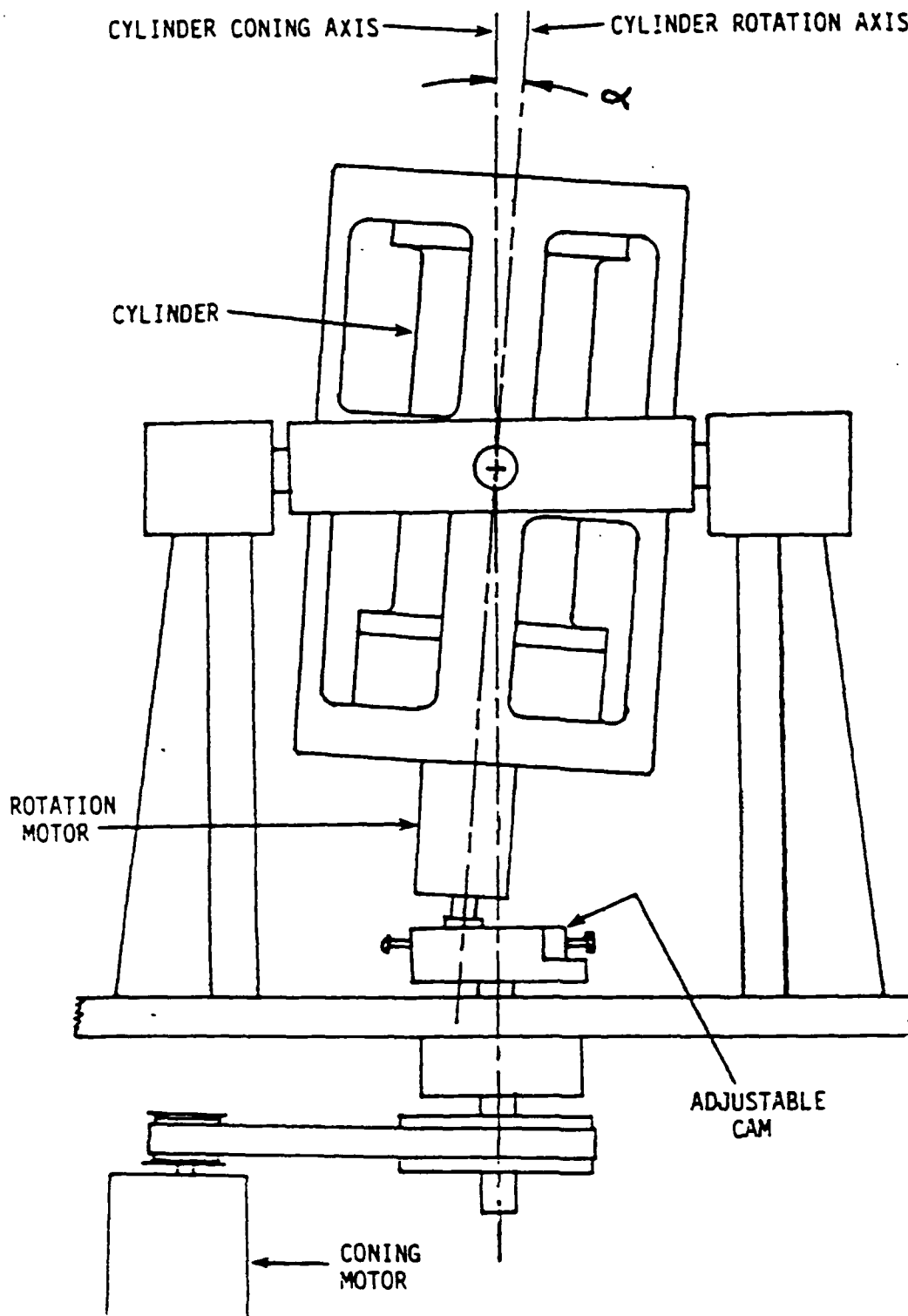


Figure 3. Forced precession gyroscope apparatus.

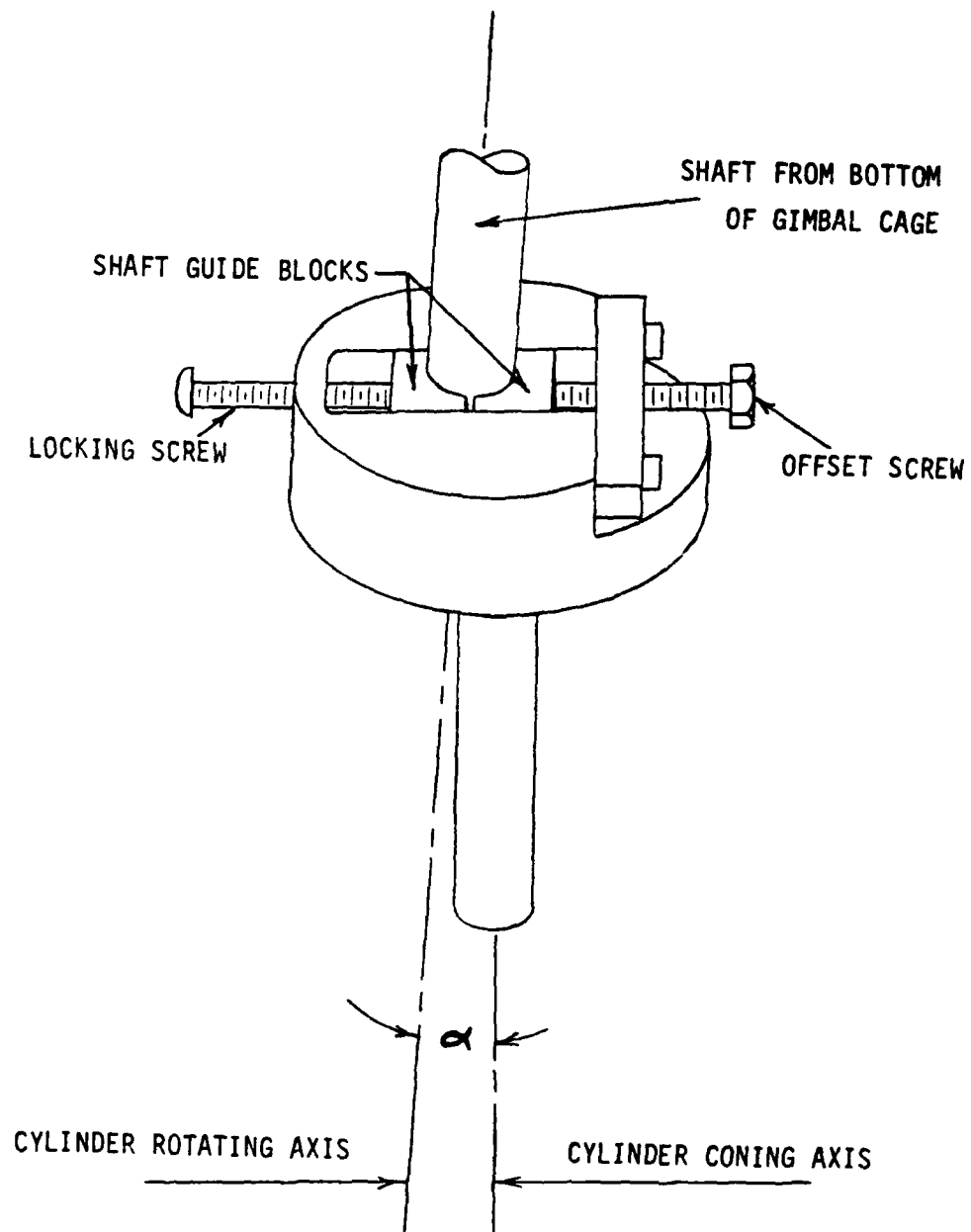


Figure 4. Precession angle adjustment cam.

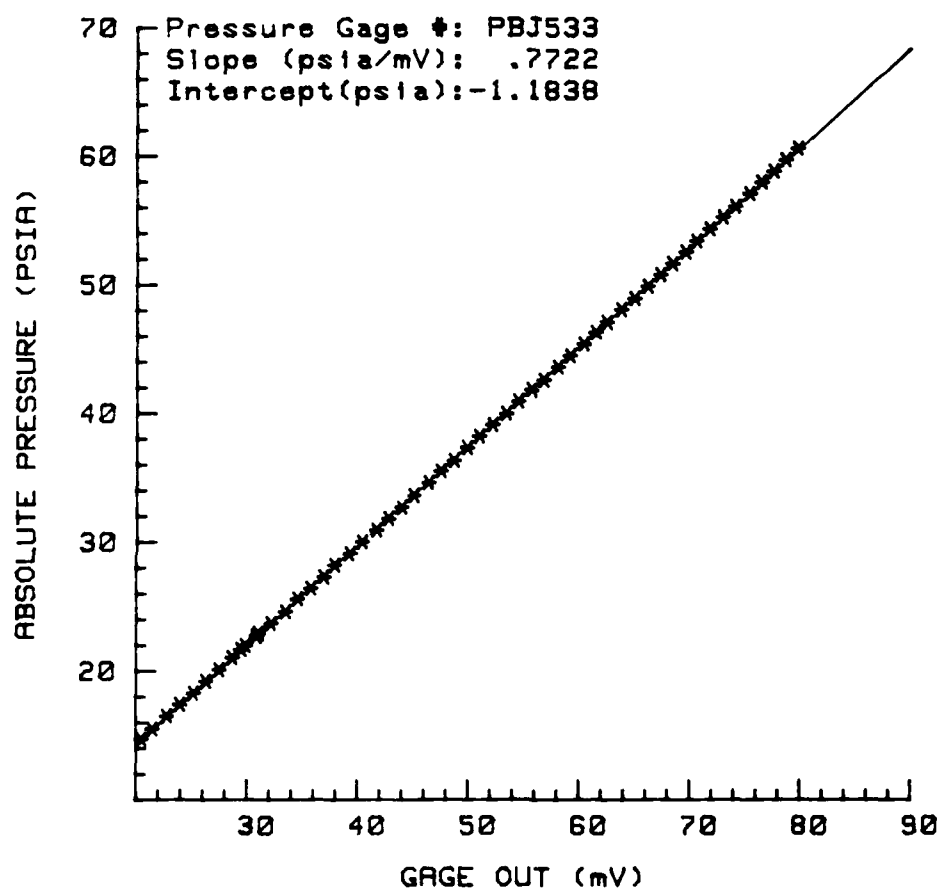


Figure 5. Pressure gage calibration for  $r/a = 0.667$ .

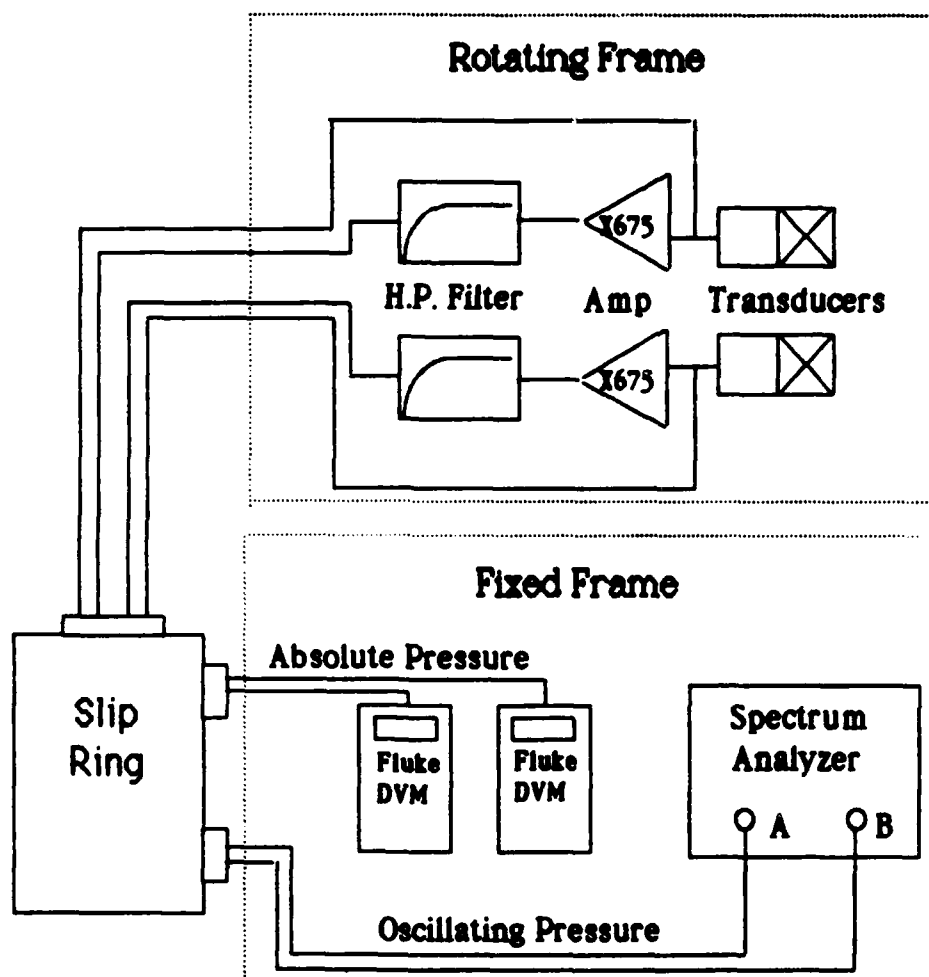


Figure 6. Instrumentation schematic.

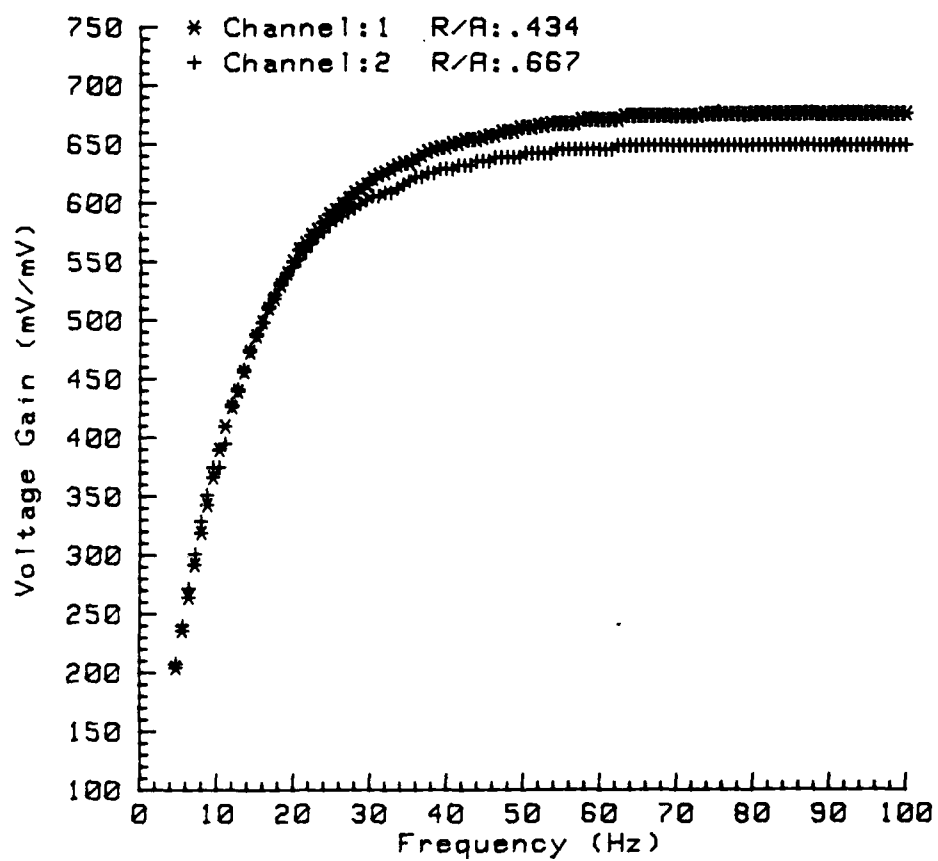


Figure 7. High pass filter amplifier transfer function.

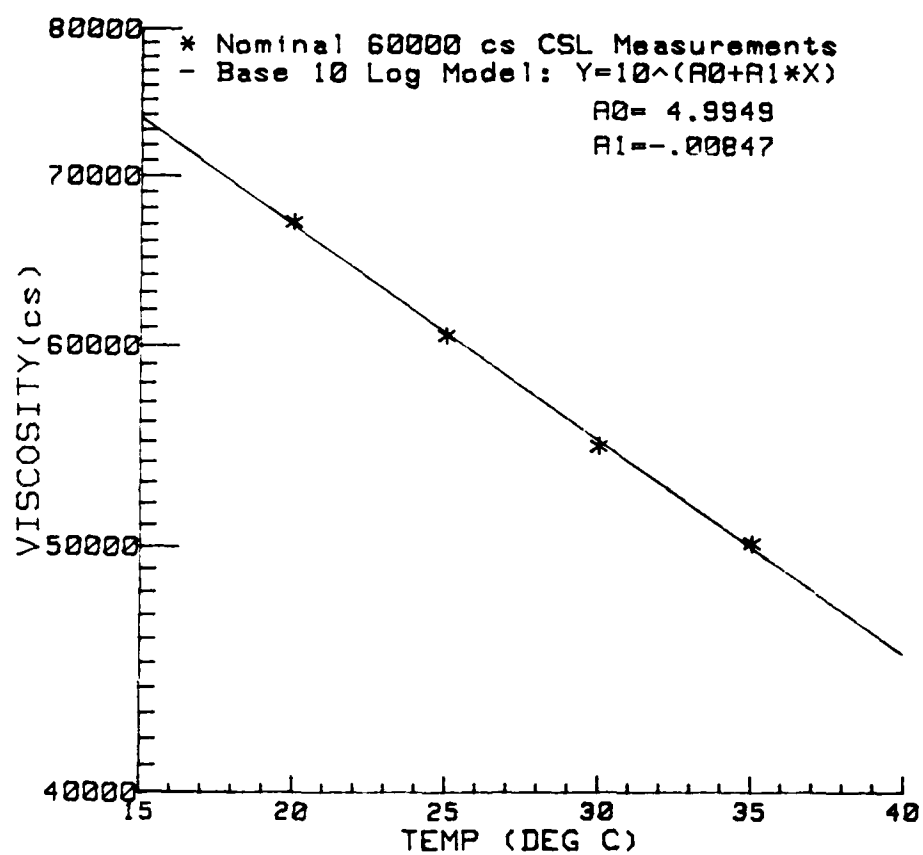


Figure 8. Liquid viscosity measurements and logarithmic function fit.

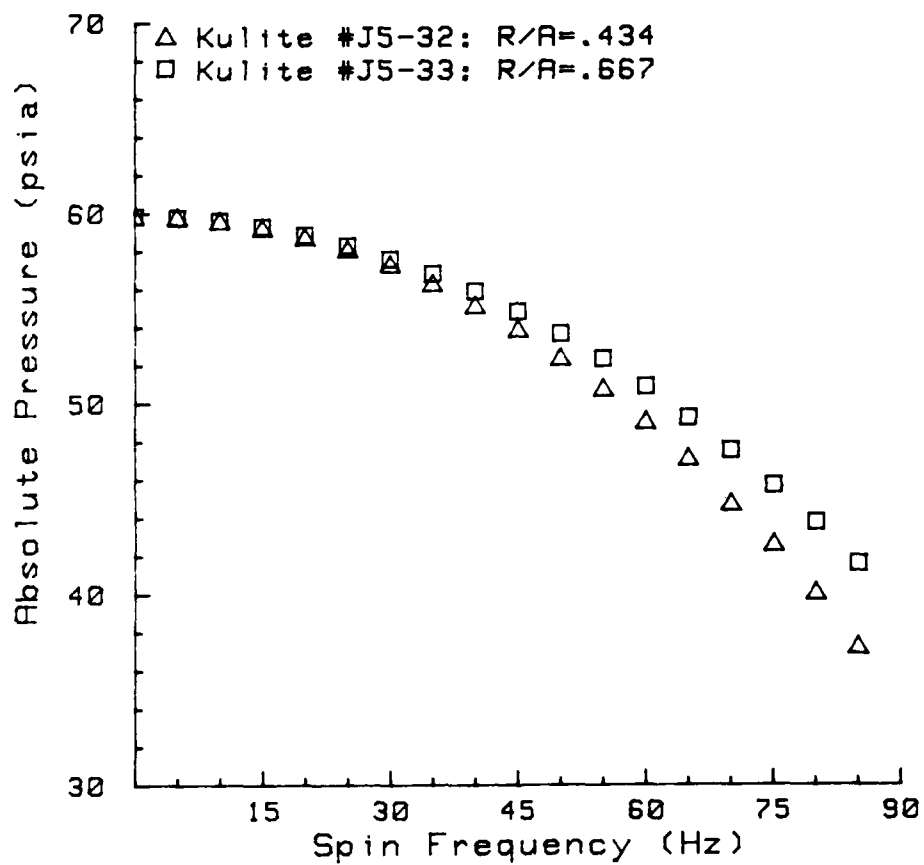


Figure 9. Absolute pressure decrease on an end wall for a slow spin-up.



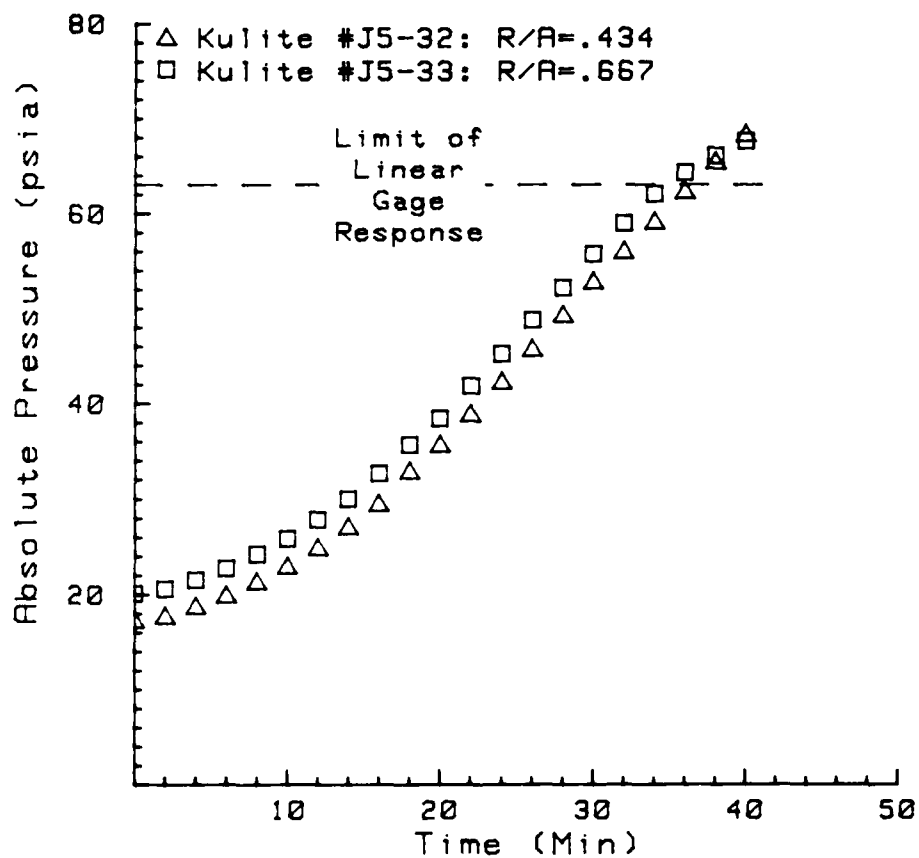


Figure 10. Absolute pressure rise for extended running time,  
(coning rate = 5 Hz, spin rate = 70 Hz).

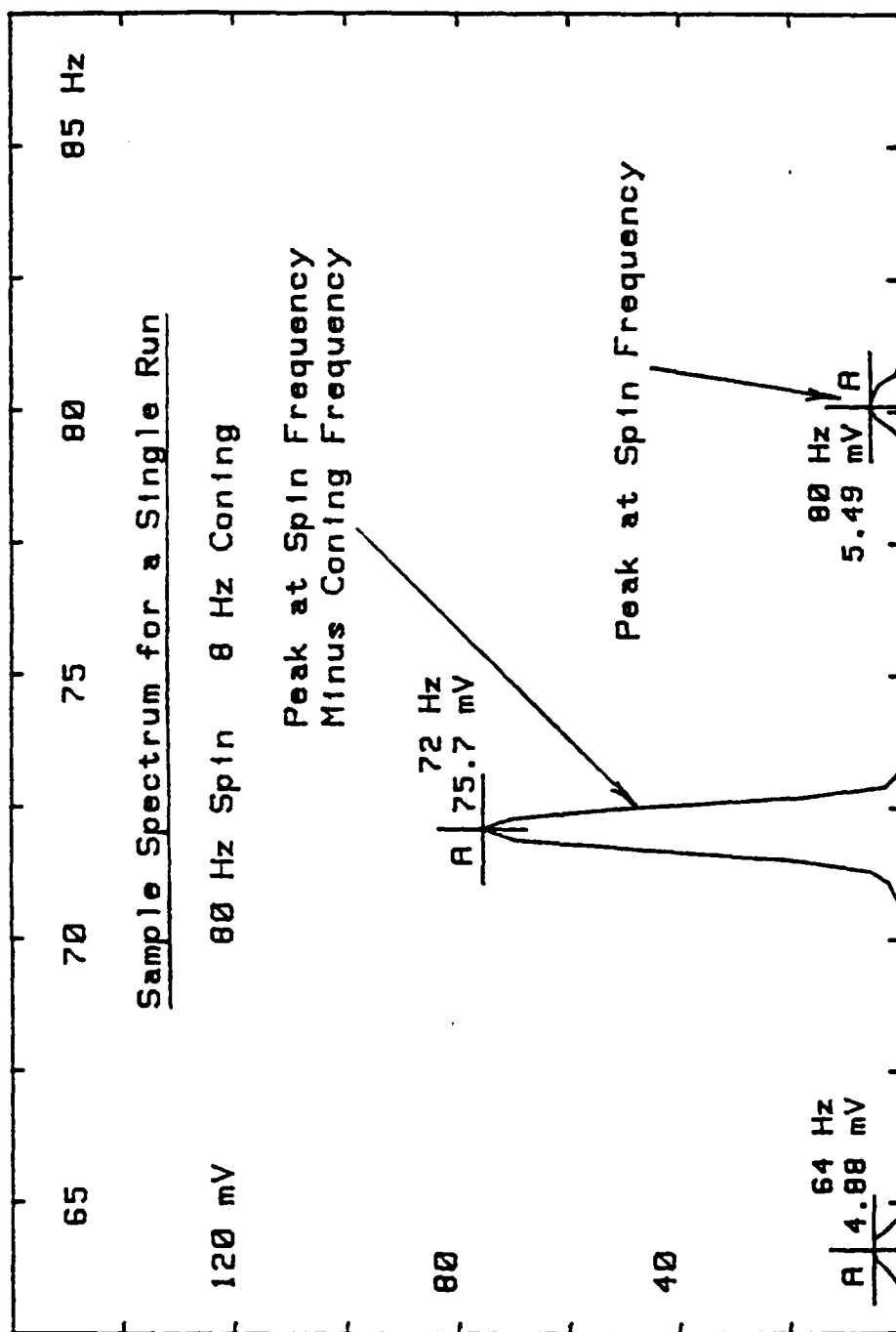


Figure 11. Spectral response for oscillatory pressures.

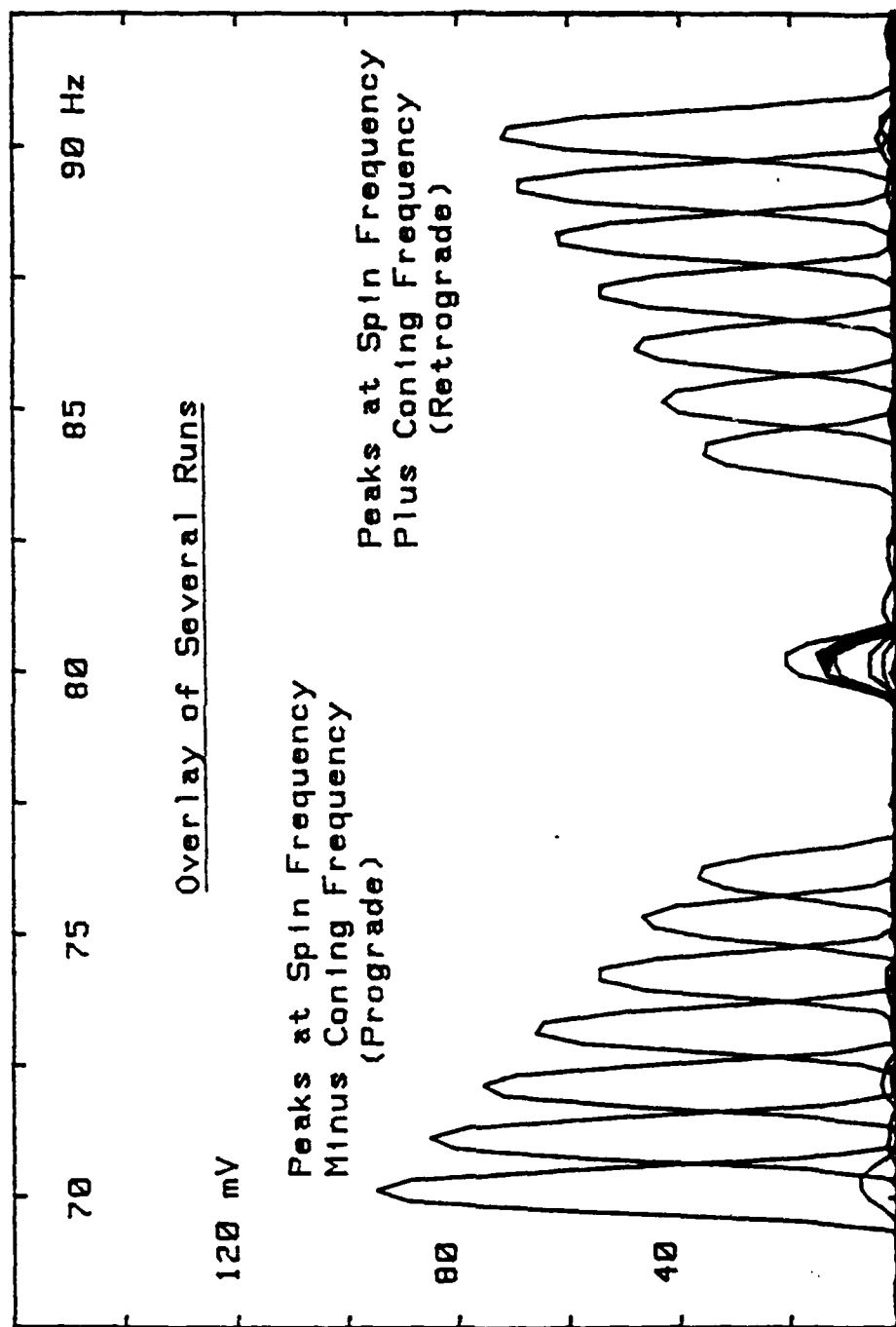


Figure 12. Spectra of several runs overlaid for low Reynolds number.

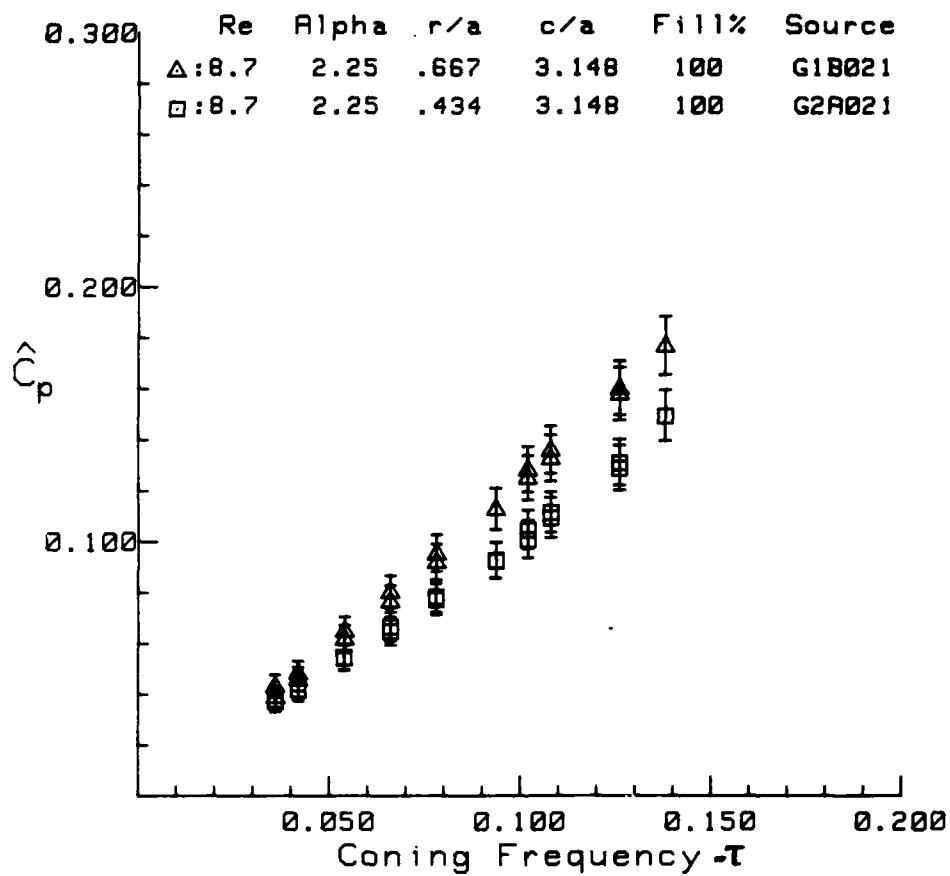


Figure 13. Prograde pressure coefficient data for two radial positions  
(r/a = 0.434 and 0.667 at Re near 8.8,  $\alpha = 2.25^\circ$ ).

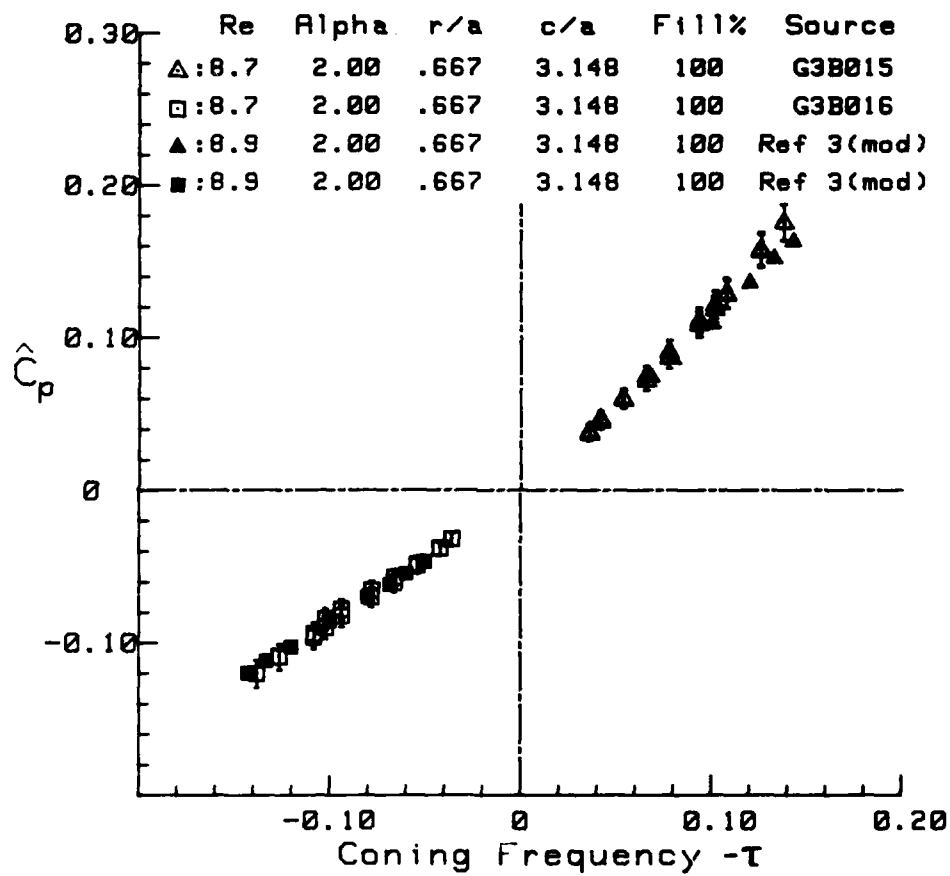


Figure 14. Prograde and retrograde pressure coefficient comparison with modified Ref. 3 data for Re near 8.8,  $\alpha = 2.00^\circ$ ,  $r/a = 0.667$ .

$Re = 80,000$     $c/a = 3.148$     $r/a = 0.667$     $x/c = 1.000$   
 Fill Ratio ( $f$ ) = 0.92

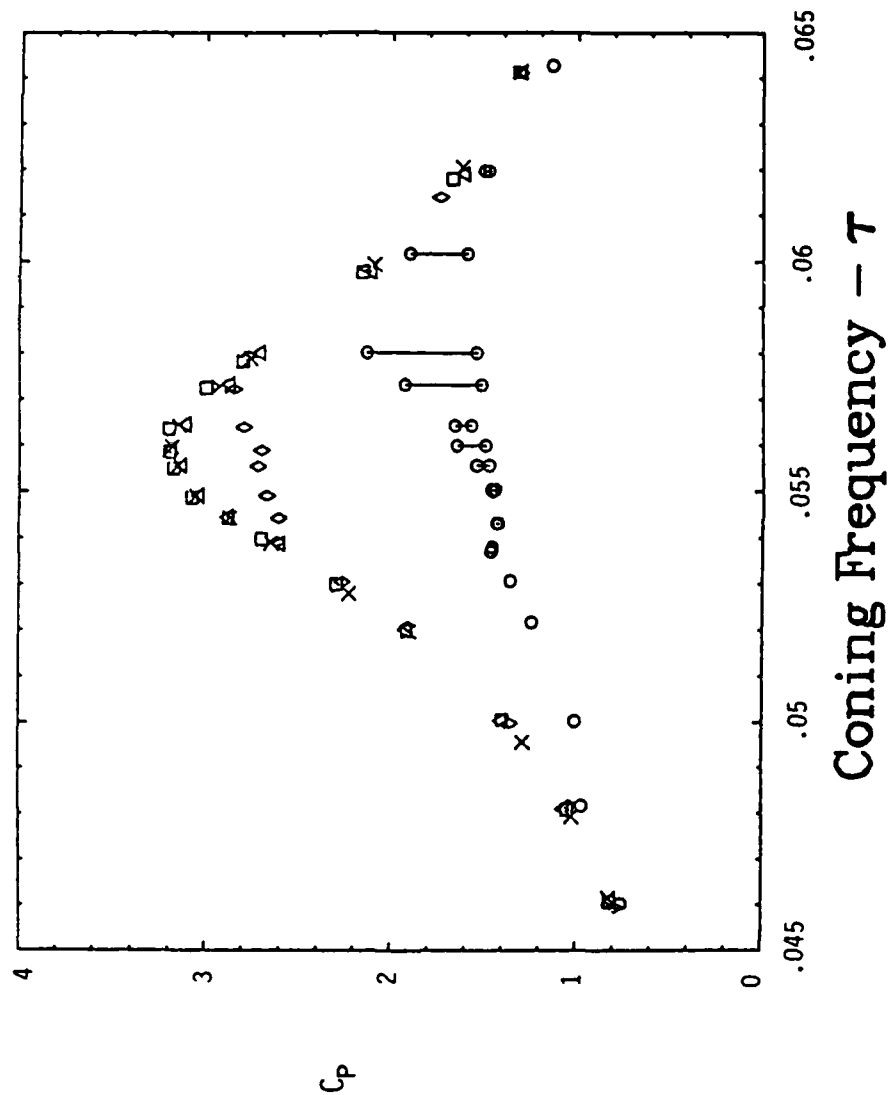


Figure 15. Experimental prograde data ( $f = .92$ );  $\Delta = 0.022^\circ$ ,  $\square = 0.051^\circ$ ,  
 $\times = 0.105^\circ$ ,  $\diamond = 0.22^\circ$ ,  $\circ = 0.50^\circ$  (Ref. 2).

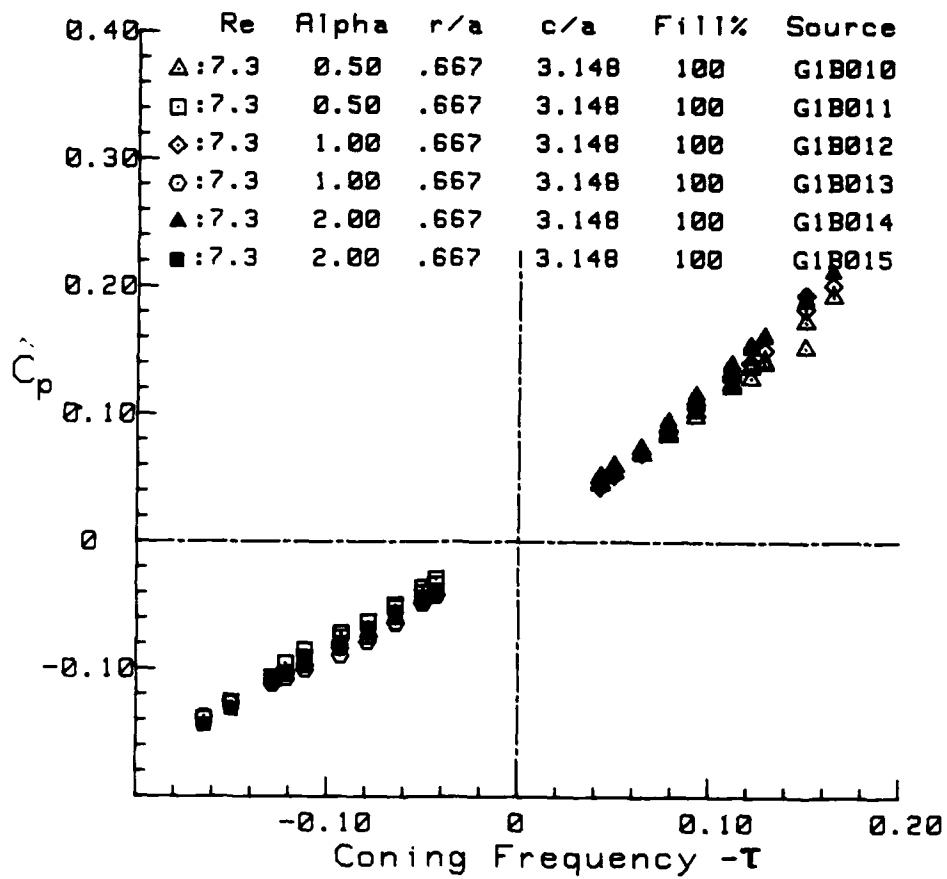


Figure 16. Prograde and retrograde pressure coefficient comparison for linearity with coning angle,  $Re = 7.3$ ,  $\alpha = 0.5, 1$  and  $2$  deg,  $r/a = 0.667$ .

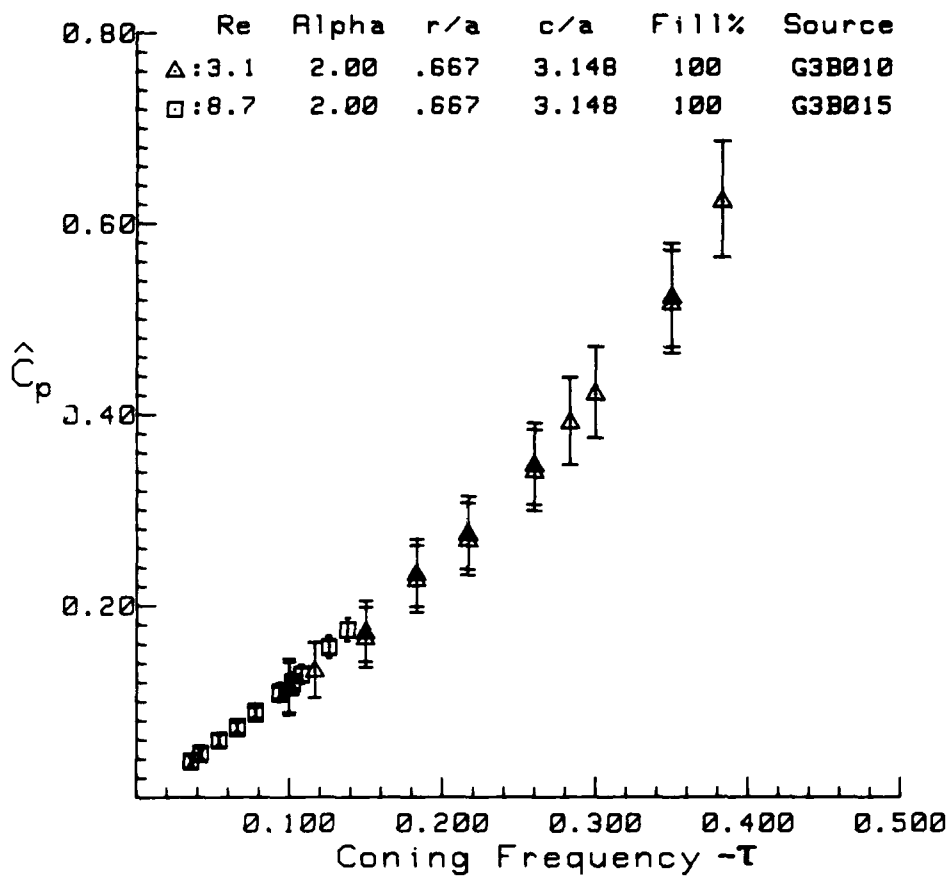


Figure 17. Expanded coning frequency and error ranges due to low spin rates.



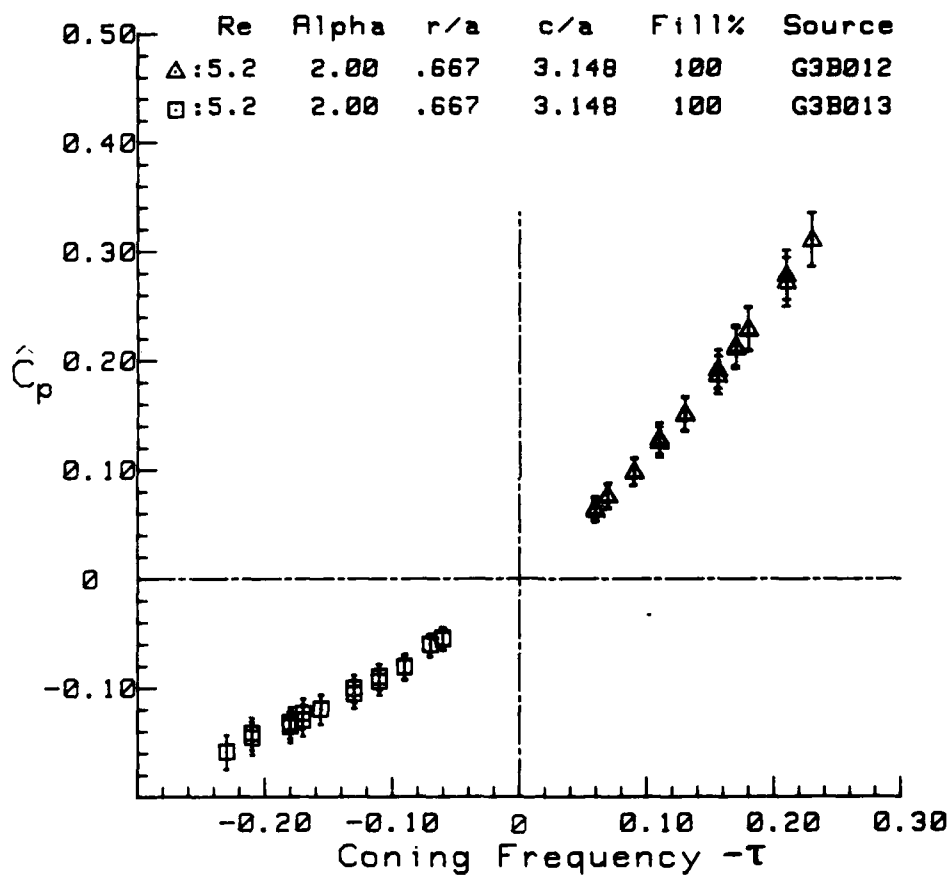


Figure 18. Prograde and retrograde pressure coefficient data for  
 $Re = 5.2, \alpha = 2.00^\circ, r/a = 0.667.$

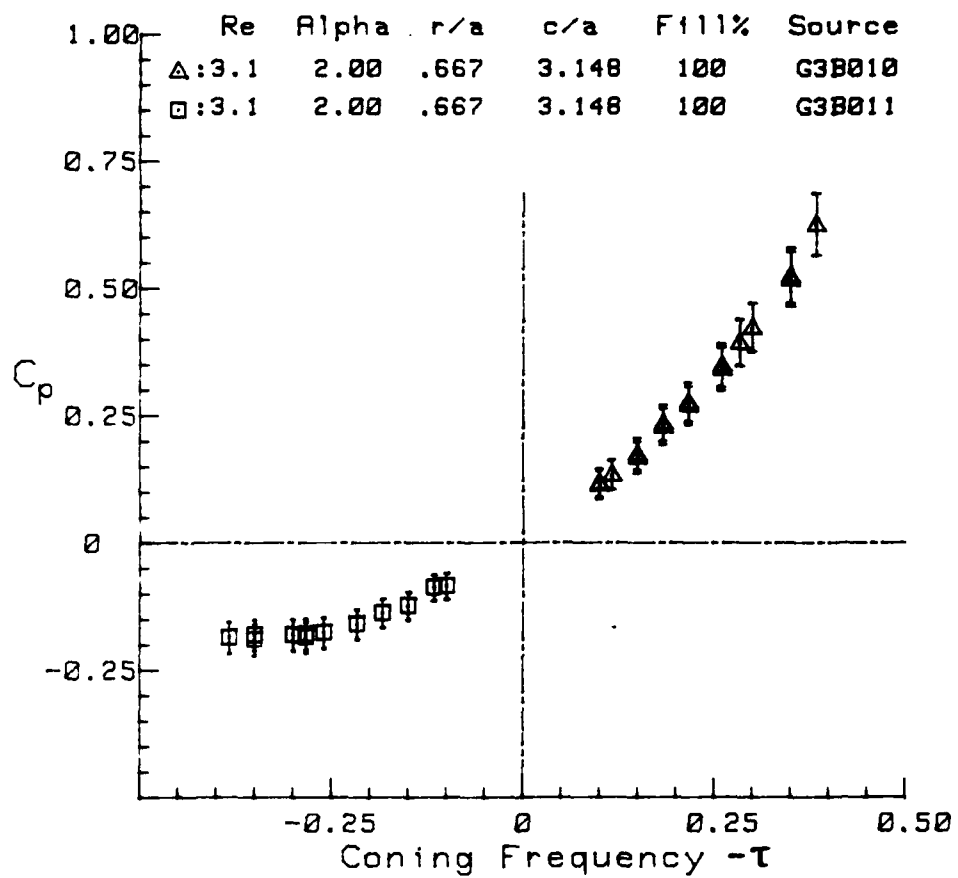


Figure 19. Prograde and retrograde pressure coefficient data for  
 $Re = 3.1$ ,  $\alpha = 2.00^\circ$ ,  $r/a = 0.667$ .

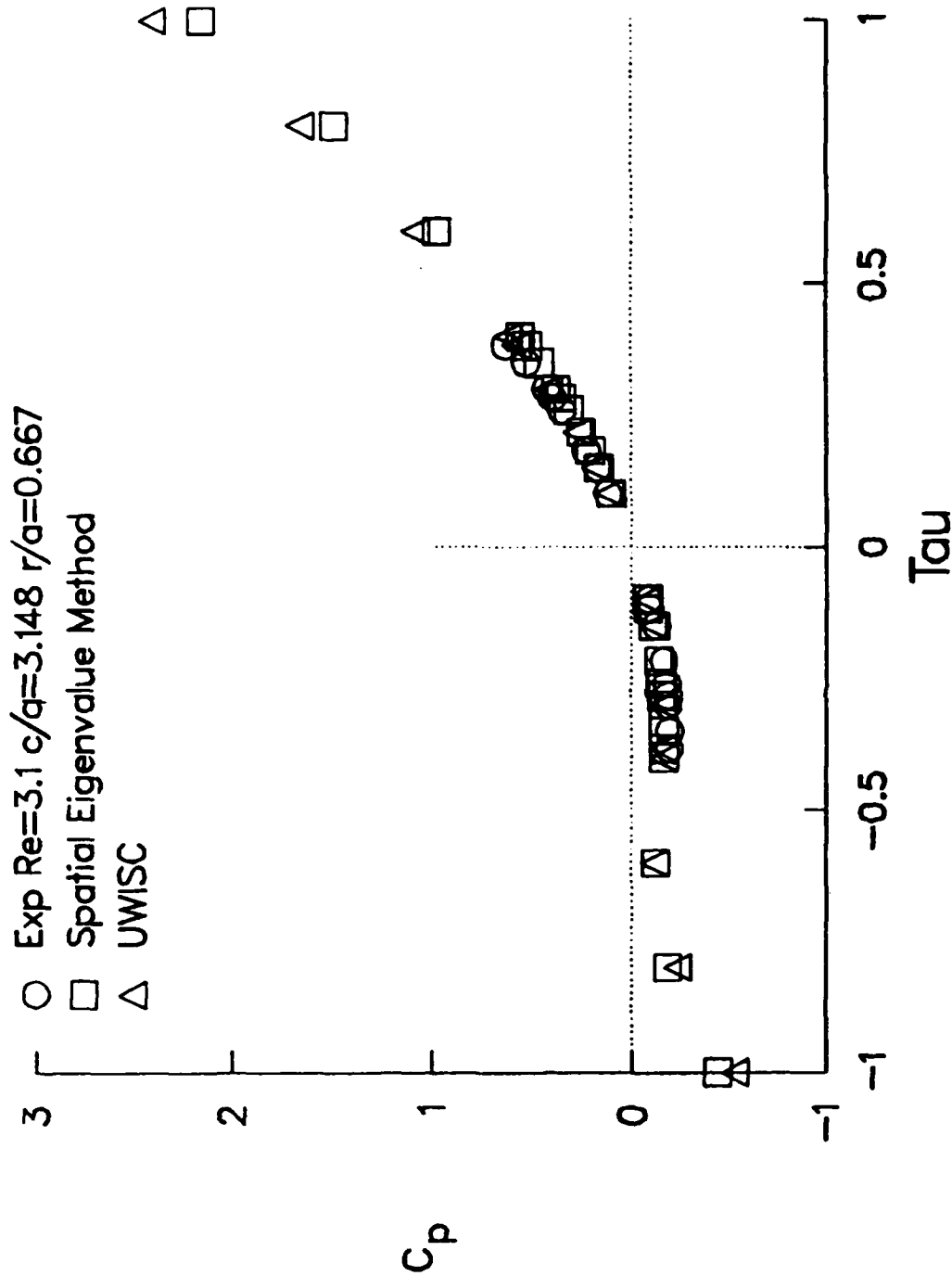


Figure 20. Comparison of experimental data to two available low Reynolds number theories for  $Re = 3.1$ .

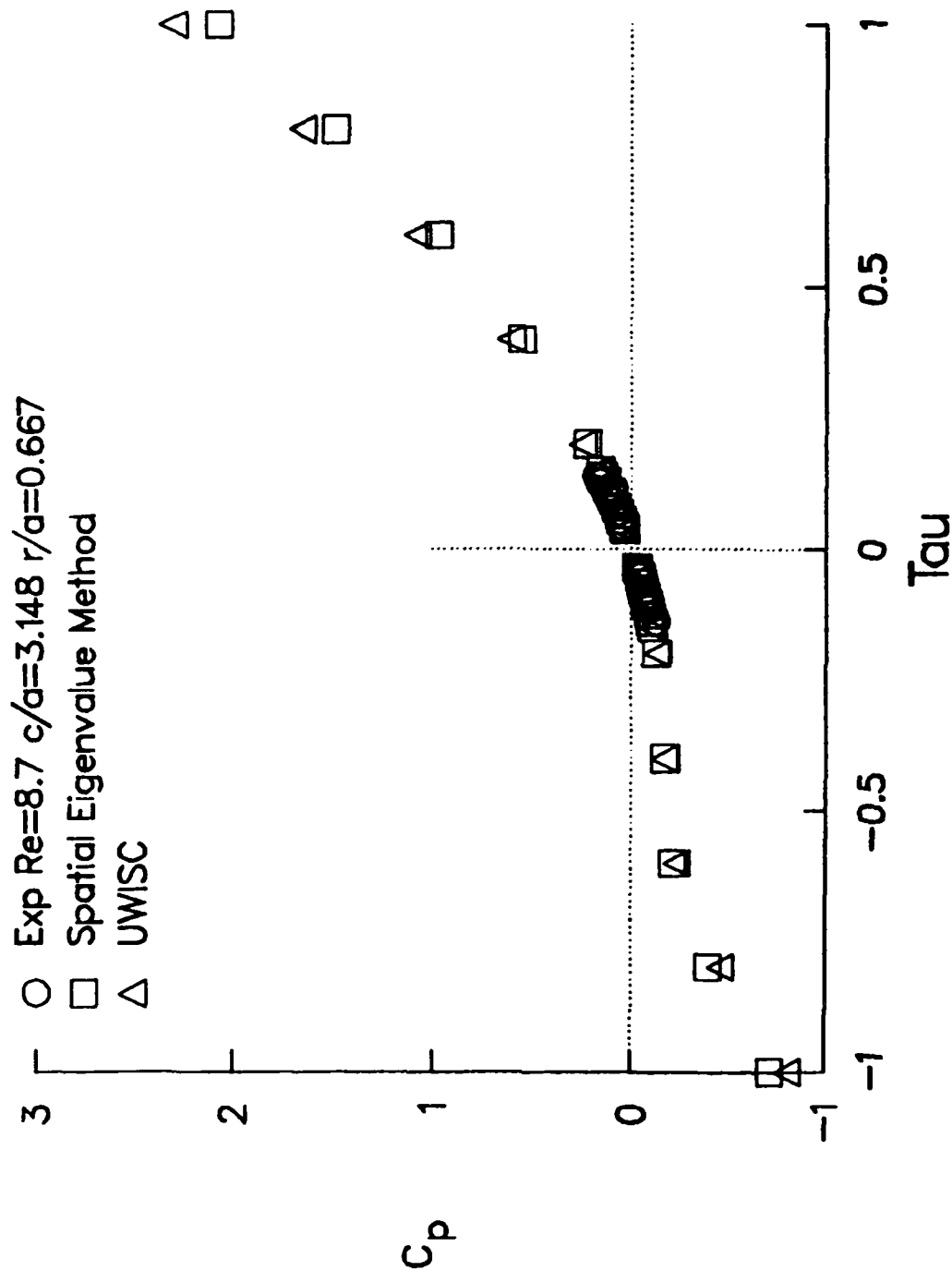


Figure 21. Comparison of experimental data to two available low Reynolds number theories for  $Re = 8.7$ .

TABLE 1. Cavity Dimensions of Lucite Cylinder with Various Inserts

	c (cm)	a (cm)	c/a	Volume (cc)
Insert #1				
Maximum	3.1838	3.1780	1.0028	202.04
Minimum	3.1802	3.1747	1.0007	201.40
Mean	3.1819	3.1761	1.0018	201.68
Insert #2				
Maximum	3.3395	3.1780	1.0519	211.92
Minimum	3.3365	3.1747	1.0499	211.30
Mean	3.3378	3.1761	1.0509	211.56
Insert #3				
Maximum	8.1949	3.1780	2.5813	520.05
Minimum	8.1923	3.1747	2.5778	518.80
Mean	8.1935	3.1761	2.5797	519.34
Insert #4				
Maximum	8.9578	3.1780	2.8216	568.46
Minimum	8.9521	3.1747	2.8169	566.92
Mean	8.9550	3.1761	2.8195	567.61
Insert #5				
Maximum	9.5292	3.1780	3.0016	604.72
Minimum	9.5259	3.1747	2.9974	603.26
Mean	9.5274	3.1761	2.9997	603.89
Insert #6				
Maximum	10.0000	3.1780	3.1499	634.60
Minimum	9.9972	3.1747	3.1457	633.10
Mean	9.9986	3.1761	3.1480	633.75

TABLE 2. Reynolds Number Calculations for Available Spin Rates and Actual Liquid Viscosities for an Internal Cylinder Radius of 3.176 cm

Reynolds Number														
20.0	1.21E+05	1.28E+03	2.42E+02	1.26E+02	13.0	2.09	1.31							
30.0	1.81E+05	1.92E+03	3.62E+02	1.88E+02	19.6	3.14	1.97							
40.0	2.41E+05	2.56E+03	4.83E+02	2.51E+02	26.1	4.19	2.62							
50.0	3.02E+05	3.19E+03	6.04E+02	3.14E+02	32.6	5.23	3.28							
60.0	3.62E+05	3.83E+03	7.25E+02	3.77E+02	39.1	6.28	3.94							
70.0	4.23E+05	4.47E+03	8.45E+02	4.40E+02	45.6	7.33	4.59							
80.0	4.83E+05	5.11E+03	9.66E+02	5.03E+02	52.2	8.37	5.25							
83.3	5.03E+05	5.32E+03	1.01E+03	5.23E+02	54.3	8.72	5.47							
Actual 25° C	1.05	99.2	524.8	1009	9720	60550	96590							
Nom Visc (cs)	1	100	500	1k	10k	60k	100k							

TABLE 3. Absolute Pressure Measurements and Predicted Pressure Differences for Constant spin rates.

ABSOLUTE PRESSURE MEASUREMENTS				
Coning (Hz)= 0		specific gravity=0.969		
Spin Rate (Hz)	r=1.38 cm Pressure (psia)	r=2.12 cm Pressure (psia)	Exp $\Delta p$ (psi)	Predicted $\Delta p$ (psi)
0	59.7	59.8	0.1	0.0
5	59.7	59.7	0.0	0.0
10	59.5	59.6	0.1	0.1
15	59.1	59.3	0.2	0.2
20	58.6	58.8	0.2	0.3
25	58.0	58.3	0.3	0.4
30	57.2	57.6	0.4	0.6
35	56.2	56.8	0.6	0.9
40	55.0	55.9	0.9	1.1
45	53.8	54.8	1.0	1.5
50	52.3	53.6	1.3	1.8
55	50.7	52.3	1.6	2.2
60	48.9	50.9	2.0	2.6
65	47.0	49.2	2.2	3.0
70	44.6	47.5	2.9	3.5
75	42.5	45.7	3.2	4.0
80	40.0	43.8	3.8	4.6
85	37.1	41.6	4.5	5.2

TABLE 4. Absolute Pressure Measurements for Constant Spin  
(70 Hz) and Coning Motion (5 Hz)

ABSOLUTE PRESSURE MEASUREMENTS					RE:7.3
SPIN(Hz):70		CONING(Hz):5		C/A:3.148	VISC(cs):60000
TIME (min)	KUJ532	R. A: .434	KUJ533	R/A: .667	
	Voltage(mV)	Pressure(psia)	Voltage(mV)	Pressure(psia)	
0	19.8	17.1	27.5	20.1	
2	20.4	17.6	28.2	20.6	
4	21.7	18.6	29.4	21.5	
6	23.2	19.7	31.0	22.8	
8	25.0	21.1	32.9	24.2	
10	27.1	22.8	35.0	25.8	
12	29.6	24.7	37.6	27.9	
14	32.4	26.9	40.4	30.0	
16	35.5	29.3	43.8	32.6	
18	39.8	32.7	47.7	35.6	
20	43.4	35.5	51.3	38.4	
22	47.5	38.7	55.7	41.8	
24	51.9	42.1	60.1	45.2	
26	56.3	45.6	64.7	48.8	
28	60.9	49.1	69.1	52.2	
30	65.4	52.7	73.7	55.7	
32	69.5	55.8	77.9	59.0	
34	73.5	59.0	81.9	62.1	
36	77.6	62.2	84.8	64.3	
38	81.6	65.3	87.1	66.1	
40	85.3	68.2	89.1	67.6	



TABLE 5. Forced Precession Gyroscope System Errors

FORCED PRECESSION GYROSCOPE SYSTEM ERRORS		
Parameter	Range	Error
Coning Rate	25-12 Hz	+/- 0.1 Hz
Spin Rate	30.0-83.3 Hz	+/- 0.15 Hz
Cylinder Radius	3.1761 cm	+/- 0.0012 cm
Cylinder 1/2 Ht	9.9986 cm	+/- 0.0014 cm
Fluid Viscosity	60600 cs	+/- 4.0 %
Fluid Density	0.969g/cc	+/- 1.0%
Coning Angle	5/1/2deg	+/- 0.021 deg
Pressure Signal	10.0-145 mV rms	+/- 2.0 mV rms
Signal Gain	450-675	+/- 2%
Pressure cal	0.7798/.7722 psi/mV	+/- 0.2%
Pressure Incpt	1.652/-1.184 psia	+/- 2.0%

TABLE 6a. Prograde Oscillatory Pressure Data for Re = 8.7,  $\alpha = 2.25^\circ$ ,  $r/a = 0.667$

File Name: GLB021    Spin Freq(Hz): 83.3    Aspct Rat(C/A): 3.148    Fill Ratio(%): 100 Gage ID Num: 33    Slope(psi/mV): .7722    Intrcpt(psi): -1.1838    Position (mm): 21.2 Radius (mm): 31.8    Pos/Rad (R/A): .667    Coning Ang(deg): 2.25    Channl Id Num: 2 Room(deg C): 25.0    Viscosity(cs): 60K    Density(gm/cc): .969    Reynolds Num: 8.7 Cyl Type: Lucite    Motion: Prograde    Gage Volt(V DC): 10.0									
Run	Coning Rate (Hz)	Tau	Amplitude (Volts rms)	Voltage Gain	Pressure Dynes/cm <sup>2</sup>	Min $\hat{C}_p$	$\hat{C}_p$	Max $\hat{C}_p$	
1	3.00	0.036	0.0389	649	4.50E+03	0.039	0.043	0.048	
2	3.50	0.042	0.0436	649	5.05E+03	0.044	0.048	0.053	
3	4.50	0.054	0.0586	649	6.79E+03	0.059	0.065	0.071	
4	5.50	0.066	0.0726	649	8.41E+03	0.074	0.080	0.087	
5	6.50	0.078	0.0862	649	9.98E+03	0.088	0.095	0.103	
6	7.80	0.094	0.1020	649	1.18E+04	0.105	0.113	0.121	
7	8.50	0.102	0.1160	649	1.34E+04	0.119	0.128	0.137	
8	9.00	0.108	0.1230	649	1.42E+04	0.127	0.136	0.145	
9	10.50	0.126	0.1450	649	1.68E+04	0.150	0.160	0.171	
10	11.50	0.138	0.1600	649	1.85E+04	0.165	0.177	0.188	
11	10.50	0.126	0.1430	649	1.66E+04	0.148	0.158	0.169	
12	9.00	0.108	0.1200	649	1.39E+04	0.124	0.132	0.142	
13	8.50	0.102	0.1130	649	1.31E+04	0.116	0.125	0.134	
14	7.80	0.094	0.1020	649	1.18E+04	0.105	0.113	0.121	
15	6.50	0.078	0.0831	649	9.62E+03	0.085	0.092	0.099	
16	5.50	0.066	0.0692	649	8.01E+03	0.070	0.076	0.083	
17	4.50	0.054	0.0558	649	6.46E+03	0.056	0.062	0.067	
18	3.50	0.042	0.0415	649	4.81E+03	0.041	0.046	0.051	
19	3.00	0.036	0.0351	649	4.06E+03	0.035	0.039	0.043	

TABLE 6b. Prograde Oscillatory Pressure Data for  $Re = 8.7$ ,  $\alpha = 2.25^\circ$ ,  $r/a = 0.434$

File Name:G2A021 Spin Freq(Hz): 83.3 Aspct Rat(C/A):3.148 Fill Ratio(%):100 Gage ID Num: 32 Slope(psi/mV):.7798 Intrcpt(psi): 1.6518 Position (mm):13.8 Radius (mm):31.8 Pos/Rad (R/A): .434 Coning Ang(deg):2.25 Channl Id Num:1 Room(deg C):25.0 Viscosity(cs): 60K Density(gm/cc): .969 Reynolds Num:8.7 Cyl Type: Lucite Motion:Prograde Gage Volt(V DC):10.0									
Run	Coning Rate (Hz)	Tau	Amplitude (Volts rms)	Voltage Gain	Pressure Dynes/cm <sup>2</sup>	Min $\hat{C}_p$	$\hat{C}_p$	Max $\hat{C}_p$	
1	3.00	0.036	0.0345	676	3.87E+03	0.033	0.037	0.041	
2	3.50	0.042	0.0387	676	4.35E+03	0.037	0.041	0.046	
3	4.50	0.054	0.0509	676	5.72E+03	0.050	0.054	0.060	
4	5.50	0.066	0.0621	676	6.97E+03	0.061	0.066	0.072	
5	6.50	0.078	0.0731	676	8.21E+03	0.072	0.078	0.085	
6	7.80	0.094	0.0863	676	9.69E+03	0.086	0.092	0.100	
7	8.50	0.102	0.0976	676	1.10E+04	0.097	0.104	0.112	
8	9.00	0.108	0.1040	676	1.17E+04	0.104	0.111	0.120	
9	10.50	0.126	0.1220	674	1.37E+04	0.122	0.131	0.140	
10	11.50	0.138	0.1390	674	1.56E+04	0.139	0.149	0.159	
11	10.50	0.126	0.1200	674	1.35E+04	0.120	0.129	0.138	
12	9.00	0.108	0.1020	676	1.15E+04	0.102	0.109	0.117	
13	8.50	0.102	0.0940	676	1.06E+04	0.093	0.101	0.108	
14	7.80	0.094	0.0865	676	9.71E+03	0.086	0.093	0.100	
15	6.50	0.078	0.0720	676	8.09E+03	0.071	0.077	0.083	
16	5.50	0.066	0.0604	676	6.78E+03	0.059	0.065	0.070	
17	4.50	0.054	0.0506	676	5.68E+03	0.049	0.054	0.059	
18	3.50	0.042	0.0391	676	4.39E+03	0.038	0.042	0.046	
19	3.00	0.036	0.0349	676	3.92E+03	0.033	0.037	0.042	

TABLE 7a. Prograde Oscillatory Pressure Data for Re = 8.7,  $\alpha = 2.00^\circ$ ,  $r/a = 0.667$

File Name:G3B015    Spin Freq(Hz): 83.3    Aspct Rat(C/A):3.148    Fill Ratio(%):100 Gage ID Num: 33    Slope(psi/mV):.7722    Intrcpt(psi):-1.1838    Position (mm):21.2 Radius (mm):31.8    Pos/Rad (R/A): .667    Coning Ang(deg):2.00    Channl Id Num:2 Room(deg C):25.0    Viscosity(cs): 60K    Density(gm/cc): .969    Reynolds Num:8.7 Cyl Type: Lucite    Motion:Prograde    Gage Volt(V DC):10.0									
Run	Coning Rate (Hz)	Tau	Amplitude (Volts rms)	Voltage Gain	Pressure Dynes/cm^2	Min Cp	Cp	Max Cp	
1	3.00	0.036	0.0308	649	3.57E+03	0.034	0.038	0.043	
2	3.50	0.042	0.0375	649	4.34E+03	0.042	0.047	0.052	
3	4.50	0.054	0.0485	649	5.62E+03	0.055	0.060	0.066	
4	5.50	0.066	0.0601	649	6.96E+03	0.068	0.075	0.081	
5	6.50	0.078	0.0729	649	8.44E+03	0.083	0.090	0.098	
6	7.80	0.094	0.0894	649	1.04E+04	0.103	0.111	0.120	
7	8.50	0.102	0.0977	649	1.13E+04	0.113	0.121	0.131	
8	9.00	0.108	0.1040	649	1.20E+04	0.120	0.129	0.139	
9	10.50	0.126	0.1270	649	1.47E+04	0.147	0.158	0.169	
10	11.50	0.138	0.1410	649	1.63E+04	0.164	0.175	0.187	
11	10.50	0.126	0.1260	649	1.46E+04	0.146	0.156	0.168	
12	9.00	0.108	0.1030	649	1.19E+04	0.119	0.128	0.138	
13	8.50	0.102	0.0952	649	1.10E+04	0.110	0.118	0.127	
14	7.80	0.094	0.0873	649	1.01E+04	0.100	0.108	0.117	
15	6.50	0.078	0.0699	649	8.09E+03	0.080	0.087	0.094	
16	5.50	0.066	0.0577	649	6.68E+03	0.066	0.072	0.078	
17	4.50	0.054	0.0476	649	5.51E+03	0.054	0.059	0.065	
18	3.50	0.042	0.0360	649	4.17E+03	0.040	0.045	0.050	
19	3.00	0.036	0.0296	649	3.43E+03	0.032	0.037	0.041	

TABLE 7b. Retrograde Oscillatory Pressure Data for Re = 8.7,  $\alpha = 2.00^\circ$ ,  $r/a = 0.667$

File Name:G3B016    Spin Freq(Hz): 83.3    Aspct Rat(C/A):3.148    Fill Ratio(%):100 Gage ID Num: 33    Slope(psi/mV):.7722    Intrcpt(psi):-1.1838    Position (mm):21.2 Radius (mm):31.8    Pos/Rad (R/A): .667    Coning Ang(deg):2.00    Channl Id Num:2 Room(deg C):25.0    Viscosity(cs): 60K    Density(gm/cc): .969    Reynolds Num:8.7 Cyl Type: Lucite    Motion:Retrograde    Gage Volt(V DC):10.0									
Run	Coning Rate (Hz)	Tau	Amplitude (Volts rms)	Voltage Gain	Pressure Dynes/cm^2	Min Cp	Cp	Max Cp	
1	-3.00	-0.036	0.0259	649	3.00E+03	-0.037	-0.032	-0.028	
2	-3.50	-0.042	0.0308	649	3.57E+03	-0.043	-0.038	-0.034	
3	-4.50	-0.054	0.0400	649	4.63E+03	-0.055	-0.050	-0.045	
4	-5.50	-0.066	0.0491	649	5.69E+03	-0.067	-0.061	-0.055	
5	-6.50	-0.078	0.0565	649	6.54E+03	-0.077	-0.070	-0.064	
6	-7.80	-0.094	0.0665	649	7.70E+03	-0.090	-0.083	-0.076	
7	-8.50	-0.102	0.0726	649	8.41E+03	-0.098	-0.090	-0.083	
8	-9.00	-0.108	0.0778	649	9.01E+03	-0.105	-0.097	-0.089	
9	-10.50	-0.126	0.0882	649	1.02E+04	-0.118	-0.109	-0.101	
10	-11.50	-0.138	0.0970	649	1.12E+04	-0.130	-0.120	-0.112	
11	-10.50	-0.126	0.0879	649	1.02E+04	-0.118	-0.109	-0.101	
12	-9.00	-0.108	0.0760	649	8.80E+03	-0.102	-0.094	-0.087	
13	-8.50	-0.102	0.0680	649	7.87E+03	-0.092	-0.084	-0.078	
14	-7.80	-0.094	0.0629	649	7.28E+03	-0.085	-0.078	-0.072	
15	-6.50	-0.078	0.0528	649	6.11E+03	-0.072	-0.066	-0.060	
16	-5.50	-0.066	0.0461	649	5.34E+03	-0.063	-0.057	-0.052	
17	-4.50	-0.054	0.0391	649	4.53E+03	-0.054	-0.049	-0.044	
18	-3.50	-0.042	0.0308	649	3.57E+03	-0.043	-0.038	-0.034	
19	-3.00	-0.036	0.0259	649	3.00E+03	-0.037	-0.032	-0.028	

TABLE 8a. Prograde Oscillatory Pressure Data for Re = 7.3,  $\alpha = 0.50^\circ$ ,  $r/a = 0.667$

File Name:GLB010										Spin Freq(Hz): 70.0		Aspct Rat(C/A):3.148		Fill Ratio(%):100	
Gage ID Num: 33		Slope(psi/mV):.7722		Intrcpt(psi):-1.1838		Position (mm):21.2									
Radius (mm):31.8		Pos/Rad (R/A): .667		Coning Ang(deg): .50		Channl Id Num:2									
Room(deg C):25.0		Viscosity(cs): 60K		Density(gm/cc): .969		Reynolds Num:7.3									
Cyl Type: Lucite		Motion:Prograde		Gage Volt(V DC):10.0											
Run	Coning Rate (Hz)	Tau	Amplitude (Volts rms)	Voltage Gain	Pressure Dynes/cm^2	Min Cp	Cp	Max Cp							
1	3.00	0.043	0.0067	649	7.71E+02	0.030	0.047	0.066							
2	3.50	0.050	0.0077	649	8.94E+02	0.037	0.054	0.074							
3	4.50	0.064	0.0099	649	1.15E+03	0.051	0.070	0.092							
4	5.50	0.079	0.0122	649	1.41E+03	0.066	0.086	0.109							
5	6.50	0.093	0.0146	649	1.69E+03	0.081	0.103	0.127							
6	7.80	0.111	0.0177	648	2.05E+03	0.102	0.125	0.151							
7	8.50	0.121	0.0194	645	2.26E+03	0.113	0.137	0.165							
8	9.00	0.129	0.0201	645	2.34E+03	0.118	0.142	0.170							
9	10.50	0.150	0.0245	645	2.85E+03	0.146	0.173	0.204							
10	11.50	0.164	0.0273	645	3.18E+03	0.164	0.193	0.226							
11	10.50	0.150	0.0216	645	2.51E+03	0.127	0.153	0.182							
12	9.00	0.129	0.0198	645	2.30E+03	0.116	0.140	0.168							
13	8.50	0.121	0.0182	645	2.12E+03	0.105	0.129	0.156							
14	7.80	0.111	0.0173	648	2.01E+03	0.099	0.122	0.148							
15	6.50	0.093	0.0140	649	1.62E+03	0.078	0.098	0.123							
16	5.50	0.079	0.0119	649	1.38E+03	0.064	0.084	0.107							
17	4.50	0.064	0.0098	649	1.14E+03	0.051	0.069	0.091							
18	3.50	0.050	0.0085	649	9.83E+02	0.042	0.060	0.080							
19	3.00	0.043	0.0065	649	7.49E+02	0.029	0.045	0.065							

TABLE 8b. Retrograde Oscillatory Pressure Data for  $Re = 7.3$ ,  $\alpha = 0.50^\circ$ ,  $r/a = 0.667$

File Name: G1B011 Spin Freq(Hz): 70.0 Aspct Rat(C/A): 3.148 Fill Ratio(%): 100 Gage ID Num: 33 Slope(psi/mv): .7722 Intrcpt(psi): -1.1838 Position (mm): 21.2 Radius (mm): 31.8 Pos/Rad (R/A): .667 Coning Ang(deg): .50 Channl Id Num: 2 Room(deg C): 25.0 Viscosity(cs): 60K Density(gm/cc): .969 Reynolds Num: 7.3 Cyl Type: Lucite Motion: Retrograde Gage Volt(V DC): 10.0									
Run	Coning Rate (Hz)	Tau	Amplitude (Volts rms)	Voltage Gain	Pressure Dynes/cm <sup>2</sup>	Min $\hat{C}_p$	$\hat{C}_p$	Max $\hat{C}_p$	
1	-3.00	-0.043	0.0047	649	5.48E+02	-0.052	-0.033	-0.018	
2	-3.50	-0.050	0.0057	649	6.59E+02	-0.059	-0.040	-0.024	
3	-4.50	-0.064	0.0073	649	8.49E+02	-0.072	-0.052	-0.034	
4	-5.50	-0.079	0.0090	649	1.04E+03	-0.084	-0.063	-0.045	
5	-6.50	-0.093	0.0107	649	1.24E+03	-0.097	-0.075	-0.056	
6	-7.80	-0.111	0.0130	649	1.51E+03	-0.115	-0.091	-0.071	
7	-8.50	-0.121	0.0148	649	1.71E+03	-0.129	-0.104	-0.083	
8	-9.00	-0.129	0.0152	649	1.76E+03	-0.132	-0.107	-0.085	
9	-10.50	-0.150	0.0179	649	2.07E+03	-0.153	-0.126	-0.103	
10	-11.50	-0.164	0.0198	649	2.29E+03	-0.167	-0.139	-0.115	
11	-10.50	-0.150	0.0179	649	2.07E+03	-0.153	-0.126	-0.103	
12	-9.00	-0.129	0.0152	649	1.76E+03	-0.132	-0.107	-0.085	
13	-8.50	-0.121	0.0136	649	1.57E+03	-0.120	-0.096	-0.075	
14	-7.80	-0.111	0.0121	649	1.40E+03	-0.108	-0.085	-0.065	
15	-6.50	-0.093	0.0102	649	1.18E+03	-0.094	-0.072	-0.053	
16	-5.50	-0.079	0.0090	649	1.04E+03	-0.084	-0.063	-0.045	
17	-4.50	-0.064	0.0070	649	8.15E+02	-0.069	-0.050	-0.033	
18	-3.50	-0.050	0.0051	649	5.92E+02	-0.054	-0.036	-0.020	
19	-3.00	-0.043	0.0042	649	4.81E+02	-0.047	-0.029	-0.014	

TABLE 9a. Prograde Oscillatory Pressure Data for  $Re = 7.3$ ,  $\alpha = 1.00^\circ$ ,  $r/a = 0.667$

File Name:GLB012    Spin Freq(Hz): 70.0    Aspct Rat(C/A):3.148    Fill Ratio(%):100 Gage ID Num: 33    Slope(psi/mV):.7722    Intrcpt(psi):-1.1838    Position (mm):21.2 Radius (mm):31.8    Pos/Rad (R/A): .667    Coning Ang(deg):1.00    Channl Id Num:2 Room(deg C):25.0    Viscosity(cs): 60K    Density(gm/cc): .969    Reynolds Num:7.3 Cyl Type: Lucite    Motion:Prograde    Gage Volt(V DC):10.0									
Run	Coning Rate (Hz)	Tau	Amplitude (Volts rms)	Voltage Gain	Pressure Dynes/cm^2	Min Cp	Cp	Max Cp	
1	3.00	0.043	0.0134	649	1.55E+03	0.038	0.047	0.058	
2	3.50	0.050	0.0160	649	1.85E+03	0.046	0.056	0.068	
3	4.50	0.064	0.0199	649	2.30E+03	0.059	0.070	0.082	
4	5.50	0.079	0.0250	649	2.89E+03	0.076	0.088	0.101	
5	6.50	0.093	0.0308	649	3.57E+03	0.095	0.108	0.123	
6	7.80	0.111	0.0372	648	4.31E+03	0.116	0.131	0.147	
7	8.50	0.121	0.0399	645	4.64E+03	0.126	0.141	0.158	
8	9.00	0.129	0.0427	645	4.97E+03	0.135	0.151	0.169	
9	10.50	0.150	0.0550	645	6.40E+03	0.176	0.194	0.215	
10	11.50	0.164	0.0571	645	6.65E+03	0.183	0.202	0.223	
11	10.50	0.150	0.0519	645	6.04E+03	0.165	0.183	0.203	
12	9.00	0.129	0.0427	645	4.97E+03	0.135	0.151	0.169	
13	8.50	0.121	0.0399	645	4.64E+03	0.126	0.141	0.158	
14	7.80	0.111	0.0363	648	4.21E+03	0.113	0.128	0.144	
15	6.50	0.093	0.0298	649	3.45E+03	0.092	0.105	0.119	
16	5.50	0.079	0.0246	649	2.85E+03	0.075	0.086	0.100	
17	4.50	0.064	0.0199	649	2.30E+03	0.059	0.070	0.082	
18	3.50	0.050	0.0148	649	1.71E+03	0.042	0.052	0.063	
19	3.00	0.043	0.0123	649	1.42E+03	0.034	0.043	0.054	



TABLE 9b. Retrograde Oscillatory Pressure Data for Re = 7.3,  $\alpha = 1.00^\circ$ ,  $r/a = 0.667$

File Name:GLB013 Spin Freq(Hz): 70.0 Aspct Rat(C/A):3.148 Fill Ratio(%):100 Gage ID Num: 33 Slope(psi/mv):.7722 Intrcpt(psi):-1.1838 Position (mm):21.2 Radius (mm):31.8 Pos/Rad (R/A): .667 Coning Ang(deg):1.00 Channl Id Num:2 Room(deg C):25.0 Viscosity(cs): 60K Density(gm/cc): .969 Reynolds Num:7.3 Cyl Type: Lucite Motion:Retrograde Gage Volt(V DC):10.0									
Run	Coning Rate (Hz)	Tau	Amplitude (Volts rms)	Voltage Gain	Pressure Dynes/cm <sup>2</sup>	Min $\hat{C}_p$	$\hat{C}_p$	Max $\hat{C}_p$	
--	----	----	-----	----	-----	-----	-----	-----	
1	-3.00	-0.043	0.0117	649	1.35E+03	-0.051	-0.041	-0.032	
2	-3.50	-0.050	0.0138	649	1.60E+03	-0.059	-0.049	-0.039	
3	-4.50	-0.064	0.0183	649	2.12E+03	-0.076	-0.064	-0.054	
4	-5.50	-0.079	0.0223	649	2.58E+03	-0.091	-0.078	-0.067	
5	-6.50	-0.093	0.0254	649	2.94E+03	-0.103	-0.089	-0.077	
6	-7.80	-0.111	0.0286	649	3.31E+03	-0.115	-0.101	-0.088	
7	-8.50	-0.121	0.0306	649	3.54E+03	-0.122	-0.108	-0.094	
8	-9.00	-0.129	0.0309	649	3.58E+03	-0.123	-0.109	-0.095	
9	-10.50	-0.150	0.0361	649	4.18E+03	-0.143	-0.127	-0.112	
10	-11.50	-0.164	0.0391	649	4.53E+03	-0.154	-0.137	-0.122	
11	-10.50	-0.150	0.0358	649	4.15E+03	-0.142	-0.126	-0.111	
12	-9.00	-0.129	0.0318	649	3.68E+03	-0.127	-0.112	-0.098	
13	-8.50	-0.121	0.0294	649	3.40E+03	-0.118	-0.103	-0.090	
14	-7.80	-0.111	0.0276	649	3.20E+03	-0.111	-0.097	-0.084	
15	-6.50	-0.093	0.0236	649	2.73E+03	-0.096	-0.083	-0.071	
16	-5.50	-0.079	0.0211	649	2.44E+03	-0.087	-0.074	-0.063	
17	-4.50	-0.064	0.0179	649	2.07E+03	-0.075	-0.063	-0.052	
18	-3.50	-0.050	0.0135	649	1.56E+03	-0.058	-0.047	-0.038	
19	-3.00	-0.043	0.0120	649	1.39E+03	-0.053	-0.042	-0.033	

TABLE 10a. Prograde Oscillatory Pressure Data for Re = 7.3,  $\alpha = 2.00^\circ$ , r/a = 0.667

File Name:GLB014										Spin Freq(Hz): 70.0		Aspct Rat(C/A):3.148		Fill Ratio(%):100	
Gage ID Num: 33		Slope(psi/mv):.7722		Intrcpt(psi):-1.1838		Position (mm):21.2									
Radius (mm):31.8		Pos/Rad (R/A): .667		Coning Ang(deg):2.00		Channl Id Num:2									
Room(deg C):25.0		Viscosity(cs): 60K		Density(gm/cc): .969		Reynolds Num:7.3									
Cyl Type: Lucite		Motion:Prograde		Gage Volt(V DC):10.0											
Run	Coning Rate (Hz)	Tau	Amplitude (Volts rms)	Voltage Gain	Pressure Dynes/cm^2	Min Cp	Cp	Max Cp							
1	3.00	0.043	0.0299	649	3.46E+03	0.046	0.053	0.059							
2	3.50	0.050	0.0333	649	3.86E+03	0.052	0.059	0.066							
3	4.50	0.064	0.0427	649	4.94E+03	0.068	0.075	0.083							
4	5.50	0.079	0.0542	649	6.28E+03	0.087	0.095	0.104							
5	6.50	0.093	0.0660	649	7.64E+03	0.107	0.116	0.126							
6	7.80	0.111	0.0797	648	9.24E+03	0.130	0.140	0.152							
7	8.50	0.121	0.0877	645	1.02E+04	0.143	0.155	0.167							
8	9.00	0.129	0.0919	645	1.07E+04	0.150	0.162	0.175							
9	10.50	0.150	0.1080	645	1.26E+04	0.177	0.191	0.205							
10	11.50	0.164	0.1200	645	1.40E+04	0.198	0.212	0.228							
11	10.50	0.150	0.1070	645	1.25E+04	0.176	0.189	0.203							
12	9.00	0.129	0.0909	645	1.06E+04	0.149	0.161	0.173							
13	8.50	0.121	0.0861	645	1.00E+04	0.141	0.152	0.164							
14	7.80	0.111	0.0788	648	9.14E+03	0.128	0.139	0.150							
15	6.50	0.093	0.0644	649	7.46E+03	0.104	0.113	0.123							
16	5.50	0.079	0.0519	649	6.01E+03	0.083	0.091	0.100							
17	4.50	0.064	0.0411	649	4.76E+03	0.065	0.072	0.080							
18	3.50	0.050	0.0309	649	3.58E+03	0.048	0.054	0.061							
19	3.00	0.043	0.0265	649	3.07E+03	0.041	0.047	0.053							

TABLE 10b. Retrograde Oscillatory Pressure Data for  $Re = 7.3$ ,  $\alpha = 2.00^\circ$ ,  $r/a = 0.667$

File Name: GIB015    Spin Freq(Hz): 70.0    Aspct Rat(C/A): 3.148    Fill Ratio(%): 100 Gage ID Num: 33    Slope(psi/mV): .7722    Intrcpt(psi): -1.1838    Position (mm): 21.2 Radius (mm): 31.8    Pos/Rad (R/A): .667    Coning Ang(deg): 2.00    Channl Id Num: 2 Room(deg C): 25.0    Viscosity(cs): 60K    Density(gm/cc): .969    Reynolds Num: 7.3 Cyl Type: Lucite    Motion: Retrograde    Gage Volt(V DC): 10.0									
Run	Coning Rate (Hz)	Tau	Amplitude (Volts rms)	Voltage Gain	Pressure Dynes/cm <sup>2</sup>	Min $\hat{C}_p$	$\hat{C}_p$	Max $\hat{C}_p$	
1	-3.00	-0.043	0.0233	649	2.70E+03	-0.047	-0.041	-0.035	
2	-3.50	-0.050	0.0264	649	3.06E+03	-0.053	-0.046	-0.041	
3	-4.50	-0.064	0.0336	649	3.89E+03	-0.066	-0.059	-0.053	
4	-5.50	-0.079	0.0405	649	4.69E+03	-0.079	-0.071	-0.064	
5	-6.50	-0.093	0.0466	649	5.40E+03	-0.090	-0.082	-0.074	
6	-7.80	-0.111	0.0547	649	6.33E+03	-0.105	-0.096	-0.088	
7	-8.50	-0.121	0.0585	649	6.77E+03	-0.112	-0.103	-0.094	
8	-9.00	-0.129	0.0625	649	7.24E+03	-0.120	-0.110	-0.101	
9	-10.50	-0.150	0.0747	649	8.65E+03	-0.142	-0.131	-0.121	
10	-11.50	-0.164	0.0819	649	9.48E+03	-0.156	-0.144	-0.133	
11	-10.50	-0.150	0.0745	649	8.63E+03	-0.142	-0.131	-0.121	
12	-9.00	-0.129	0.0624	649	7.22E+03	-0.120	-0.110	-0.101	
13	-8.50	-0.121	0.0584	649	6.76E+03	-0.112	-0.103	-0.094	
14	-7.80	-0.111	0.0531	649	6.15E+03	-0.102	-0.093	-0.085	
15	-6.50	-0.093	0.0451	649	5.22E+03	-0.087	-0.079	-0.072	
16	-5.50	-0.079	0.0387	649	4.48E+03	-0.076	-0.068	-0.061	
17	-4.50	-0.064	0.0315	649	3.65E+03	-0.062	-0.055	-0.049	
18	-3.50	-0.050	0.0247	649	2.86E+03	-0.050	-0.043	-0.038	
19	-3.00	-0.043	0.0217	649	2.51E+03	-0.044	-0.038	-0.033	

TABLE 11a. Prograde Oscillatory Pressure Data for Re = 5.2,  $\alpha = 2.00^\circ$ , r/a = 0.667

File Name:G3B012 Spin Freq(Hz): 50.0 Aspct Rat(C/A):3.148 Fill Ratio(%):100 Gage ID Num: 33 Slope(psi/mV):.7722 Intrcpt(psi):-1.1838 Position (mm):21.2 Radius (mm):31.8 Pos/Rad (R/A): .667 Coning Ang(deg):2.00 Channl Id Num:2 Room(deg C):25.0 Viscosity(cs): 60K Density(gm/cc): .969 Reynolds Num:5.2 Cyl Type: Lucite Motion:Prograde Gage Volt(V DC):10.0									
Run	Coning Rate (Hz)	Tau	Amplitude (Volts rms)	Voltage Gain	Pressure Dynes/cm <sup>2</sup>	Min $\hat{C}_p$	$\hat{C}_p$	Max $\hat{C}_p$	
1	3.00	0.060	0.0183	639	2.15E+03	0.054	0.064	0.075	
2	3.50	0.070	0.0217	639	2.55E+03	0.065	0.076	0.088	
3	4.50	0.090	0.0278	635	3.29E+03	0.086	0.098	0.111	
4	5.50	0.110	0.0363	635	4.29E+03	0.114	0.128	0.143	
5	6.50	0.130	0.0427	633	5.06E+03	0.136	0.151	0.167	
6	7.80	0.156	0.0540	632	6.42E+03	0.174	0.191	0.210	
7	8.50	0.170	0.0601	632	7.15E+03	0.194	0.213	0.233	
8	9.00	0.180	0.0641	630	7.65E+03	0.209	0.228	0.248	
9	10.50	0.210	0.0763	629	9.12E+03	0.250	0.271	0.295	
10	11.50	0.230	0.0867	626	1.04E+04	0.286	0.310	0.335	
11	10.50	0.210	0.0781	629	9.33E+03	0.256	0.278	0.301	
12	9.00	0.180	0.0644	630	7.68E+03	0.210	0.229	0.249	
13	8.50	0.170	0.0595	632	7.08E+03	0.192	0.211	0.230	
14	7.80	0.156	0.0525	632	6.24E+03	0.169	0.186	0.204	
15	6.50	0.130	0.0424	633	5.03E+03	0.135	0.150	0.166	
16	5.50	0.110	0.0354	635	4.19E+03	0.111	0.125	0.139	
17	4.50	0.090	0.0275	635	3.25E+03	0.085	0.097	0.110	
18	3.50	0.070	0.0214	639	2.52E+03	0.064	0.075	0.087	
19	3.00	0.060	0.0177	639	2.08E+03	0.052	0.062	0.073	

TABLE 11b. Retrograde Oscillatory Pressure Data for Re = 5.2,  $\alpha = 2.00^\circ$ , r/a = 0.667

File Name:G3B013    Spin Freq(Hz): 50.0    Aspt Rat(C/A):3.148    Fill Ratio(%):100 Gage ID Num: 33    Slope(psi/mV):.7722    Intrcpt(psi):-1.1838    Position (mm):21.2 Radius (mm):31.8    Pos/Rad (R/A): .667    Coning Ang(deg):2.00    Channl Id Num:2 Room(deg C):25.0    Viscosity(cs): 60K    Density(gm/cc): .969    Reynolds Num:5.2 Cyl Type: Lucite    Motion:Retrograde    Gage Volt(V DC):10.0									
Run	Coning Rate (Hz)	Tau	Amplitude (Volts rms)	Voltage Gain	Pressure Dynes/cm^2	Min Cp	Cp	Max Cp	
1	-3.00	-0.060	0.0156	642	1.83E+03	-0.065	-0.054	-0.045	
2	-3.50	-0.070	0.0174	642	2.04E+03	-0.071	-0.061	-0.051	
3	-4.50	-0.090	0.0235	645	2.74E+03	-0.093	-0.081	-0.070	
4	-5.50	-0.110	0.0272	645	3.17E+03	-0.107	-0.094	-0.083	
5	-6.50	-0.130	0.0305	645	3.55E+03	-0.119	-0.106	-0.093	
6	-7.80	-0.156	0.0345	645	4.02E+03	-0.134	-0.119	-0.106	
7	-8.50	-0.170	0.0375	645	4.36E+03	-0.145	-0.130	-0.116	
8	-9.00	-0.180	0.0391	645	4.55E+03	-0.151	-0.135	-0.122	
9	-10.50	-0.210	0.0421	645	4.90E+03	-0.162	-0.146	-0.131	
10	-11.50	-0.230	0.0458	645	5.33E+03	-0.175	-0.159	-0.143	
11	-10.50	-0.210	0.0409	645	4.76E+03	-0.157	-0.142	-0.127	
12	-9.00	-0.180	0.0381	645	4.43E+03	-0.147	-0.132	-0.118	
13	-8.50	-0.170	0.0357	645	4.15E+03	-0.138	-0.124	-0.110	
14	-7.80	-0.156	0.0345	645	4.02E+03	-0.134	-0.119	-0.106	
15	-6.50	-0.130	0.0290	645	3.38E+03	-0.114	-0.100	-0.088	
16	-5.50	-0.110	0.0259	645	3.01E+03	-0.102	-0.090	-0.078	
17	-4.50	-0.090	0.0232	645	2.70E+03	-0.092	-0.080	-0.069	
18	-3.50	-0.070	0.0174	642	2.04E+03	-0.071	-0.061	-0.051	
19	-3.00	-0.060	0.0159	642	1.86E+03	-0.066	-0.055	-0.046	

TABLE 12a. Prograde Oscillatory Pressure Data for Re = 3.1,  $\alpha = 2.00^\circ$ ,  $r/a = 0.667$

File Name:G3B010 Spin Freq(Hz): 30.0 Aspct Rat(C/A):3.148 Fill Ratio(%):100									
Gage ID Num: 33 Slope(psi/mV):.7722 Intrcpt(psi):-1.1838 Position (mm):21.2									
Radius (mm):31.8 Pos/Rad (R/A): .667 Coning Ang(deg):2.00 Channl Id Num:2									
Room(deg C):25.0 Viscosity(cs): 60K Density(gm/cc): .969 Reynolds Num:3.1									
Cyl Type: Lucite Motion:Prograde Gage Volt(V DC):10.0									
Run	Coning Rate (Hz)	Tau	Amplitude (Volts rms)	Voltage Gain	Pressure Dynes/cm^2	Min Cp	Cp	Max Cp	
1	3.00	0.100	0.0110	591	1.40E+03	0.089	0.116	0.145	
2	3.50	0.117	0.0125	589	1.59E+03	0.104	0.132	0.162	
3	4.50	0.150	0.0156	585	2.00E+03	0.136	0.166	0.199	
4	5.50	0.183	0.0211	579	2.74E+03	0.193	0.226	0.263	
5	6.50	0.217	0.0253	573	3.32E+03	0.238	0.274	0.314	
6	7.80	0.260	0.0314	564	4.19E+03	0.305	0.346	0.391	
7	8.50	0.283	0.0351	558	4.73E+03	0.347	0.391	0.439	
8	9.00	0.300	0.0375	554	5.09E+03	0.375	0.421	0.471	
9	10.50	0.350	0.0455	541	6.32E+03	0.470	0.522	0.579	
10	11.50	0.383	0.0534	533	7.53E+03	0.565	0.623	0.686	
11	10.50	0.350	0.0449	541	6.24E+03	0.464	0.515	0.572	
12	9.00	0.300	0.0375	554	5.09E+03	0.375	0.421	0.471	
13	8.50	0.283	0.0351	558	4.73E+03	0.347	0.391	0.439	
14	7.80	0.260	0.0308	564	4.11E+03	0.299	0.339	0.384	
15	6.50	0.217	0.0247	573	3.24E+03	0.232	0.268	0.307	
16	5.50	0.183	0.0217	579	2.81E+03	0.199	0.233	0.270	
17	4.50	0.150	0.0162	585	2.08E+03	0.142	0.172	0.205	
18	3.50	0.117	0.0125	589	1.59E+03	0.104	0.132	0.162	
19	3.00	0.100	0.0107	591	1.36E+03	0.086	0.112	0.142	

TABLE 12b. Retrograde Oscillatory Pressure Data for Re = 3.1,  $\alpha = 2.00^\circ$ ,  $r/a = 0.667$

File Name:G33011 Spin Freq(Hz): 30.0 Aspt Pat(C/\):3.143 Fill Ratio(%):100 Gage ID Num: 33 Slope(psi/mv):.7722 Intrcpt(psi):-1.1838 Position (mm):21.2 Radius (mm):31.8 Pos/Rad (R/A): .667 Coning Ang(deg):2.00 Channl Id Num:2 Room(deg C):25.0 Viscosity(cs): 60K Density(gm/cc): .969 Reynolds Num:3.1 Cyl Type: Lucite Motion:Petrograde Gage Volt(V DC):10.0									
Run	Coning Rate (Hz)	Tau	Amplitude (Volts rms)	Voltage Gain	Pressure Dynes/cm <sup>2</sup>	Min $\hat{C}_p$	$\hat{C}_p$	Max $\hat{C}_p$	
1	-3.00	-0.100	0.0032	610	1.02E+03	-0.111	-0.084	-0.060	
2	-3.50	-0.117	0.0085	612	1.05E+03	-0.114	-0.087	-0.063	
3	-4.50	-0.150	0.0122	616	1.49E+03	-0.152	-0.123	-0.097	
4	-5.50	-0.183	0.0137	620	1.66E+03	-0.167	-0.137	-0.110	
5	-6.50	-0.217	0.0159	622	1.92E+03	-0.190	-0.159	-0.131	
6	-7.80	-0.260	0.0177	625	2.13E+03	-0.208	-0.176	-0.147	
7	-8.50	-0.283	0.0186	626	2.23E+03	-0.217	-0.185	-0.155	
8	-9.00	-0.300	0.0183	628	2.19E+03	-0.213	-0.181	-0.152	
9	-10.50	-0.350	0.0192	629	2.29E+03	-0.222	-0.190	-0.160	
10	-11.50	-0.383	0.0189	632	2.25E+03	-0.218	-0.186	-0.156	
11	-10.50	-0.350	0.0183	629	2.19E+03	-0.213	-0.181	-0.152	
12	-9.00	-0.300	0.0183	628	2.19E+03	-0.213	-0.181	-0.152	
13	-8.50	-0.283	0.0180	626	2.16E+03	-0.211	-0.179	-0.150	
14	-7.80	-0.260	0.0177	625	2.13E+03	-0.208	-0.176	-0.147	
15	-6.50	-0.217	0.0159	622	1.92E+03	-0.190	-0.159	-0.131	
16	-5.50	-0.183	0.0137	620	1.66E+03	-0.167	-0.137	-0.110	
17	-4.50	-0.150	0.0122	616	1.49E+03	-0.152	-0.123	-0.097	
18	-3.50	-0.117	0.0085	612	1.05E+03	-0.114	-0.087	-0.063	
19	-3.00	-0.100	0.0082	610	1.02E+03	-0.111	-0.084	-0.060	

TABLE 13. Comparison of Experimental Data to Two Available Low Reynolds Number Theories for  $Re = 3.1$

Reynolds Number: 3.1			
Fill Ratio (%): 100		c/a: 3.148	r/a: 0.667
TAU	EXP	SPEVM*	UWISC
-0.99999	----	-0.43679	-0.5263
-0.800	----	-0.18061	-0.2306
-0.600	----	-0.12147	-0.1180
-0.400	----	-0.15983	-0.1614
-0.383	-0.186	-0.16046	-0.1594
-0.350	-0.190	-0.16010	----
-0.300	-0.181	-0.15482	-0.1578
-0.283	-0.185	-0.15186	----
-0.260	-0.176	-0.14662	----
-0.217	-0.159	-0.13359	-0.1384
-0.183	-0.137	-0.12019	----
-0.150	-0.123	-0.10394	-0.1164
-0.117	-0.087	-0.08644	----
-0.100	-0.084	-0.07575	-0.0797
0.100	0.116	0.10025	0.1077
0.117	0.132	0.11973	----
0.150	0.166	0.15956	0.1742
0.183	0.226	0.20209	----
0.217	0.274	0.24866	0.2691
0.260	0.346	0.31164	----
0.283	0.391	0.34724	----
0.300	0.421	0.37432	0.4081
0.350	0.522	0.45818	----
0.383	0.623	0.51677	0.5668
0.400	----	0.54805	0.6045
0.600	----	0.96860	1.0750
0.800	----	1.48574	1.6560
0.99999	----	2.15680	2.4040
* Number of Eigenvalues: 10			



TABLE 14. Comparison of Experimental Data to Two Available Low Reynolds Number Theories for  $Re = 8.7$

Reynolds Number: 8.7			
Fill Ratio (%): 100		c/a: 3.148 r/a: 0.667	
TAU	EXP	SPEVM*	UWISC
-0.99999	----	-0.71524	-0.8100
-0.800	----	-0.3902	-0.4550
-0.600	----	-0.20929	-0.2303
-0.400	----	-0.16214	-0.1679
-0.200	----	-0.12099	-0.1277
-0.150	----	-0.0996	-0.1058
-0.138	-0.120	-0.09363	----
-0.126	-0.109	-0.08731	-0.0929
-0.108	-0.097	-0.07723	----
-0.102	-0.090	-0.07369	-0.0787
-0.094	-0.083	-0.06884	----
-0.078	-0.070	-0.05867	-0.0629
-0.066	-0.061	-0.05063	----
-0.054	-0.050	-0.04224	-0.0453
-0.042	-0.038	-0.03348	----
-0.036	-0.032	-0.02897	-0.0310
0.036	0.038	0.03227	0.0348
0.042	0.047	0.03797	----
0.054	0.060	0.04964	0.0537
0.066	0.075	0.06170	----
0.078	0.090	0.07412	0.0803
0.094	0.111	0.09126	----
0.102	0.121	0.09971	0.1086
0.108	0.129	0.10680	----
0.126	0.158	0.12754	0.1387
0.138	0.175	0.14183	----
0.150	----	0.15648	0.1704
0.200	----	0.22160	0.2419
0.400	----	0.54650	0.6020
0.600	----	0.97159	1.0767
0.800	----	1.49120	1.6610
0.99999	----	2.08436	2.3109
* Number of Eigenvalues: 10			

## REFERENCES

1. Sedney, R., "A Survey of the Fluid Dynamic Aspects of Liquid-Filled Projectiles," AIAA Paper No. 85-1822-CP, AIAA 12th Atmospheric Flight Mechanics Conference, August 1985.
2. Whiting, R.D., "An Experimental Study of Forced Asymmetric Oscillations in a Rotating Liquid-Filled Cylinder," ARBRL-TR-02376, U.S. Army Ballistic Research Laboratory, Aberdeen Proving Ground, Maryland, October 1981. (AD A107948)
3. Nusca, M.J., D'Amico, W.P., and Beims, W.G., "Pressure Measurements in a Rapidly Rotating and Coning, Highly Viscous Fluid," ARBRL-MR-03325, U.S. Army Ballistic Research Laboratory, Aberdeen Proving Ground, Maryland, November 1983. (AD A136824)
4. D'Amico, W.P., Jr., Beims, W.G., Rogers, T.H., "Pressure Measurements of a Rotating Liquid for Impulsive Coning Motion," ARBRL-MR-03208, U.S. Army Ballistic Research Laboratory, Aberdeen Proving Ground, Maryland, November 1982. (AD A121603)
5. D'Amico, W.P., Jr., "Instabilities of a Gyroscope Produced by Rapidly Rotating, Highly Viscous Liquids," ARBRL-MR-03285, U.S. Army Ballistic Research Laboratory, Aberdeen Proving Ground, Maryland, June 1983. (AD A130874)
6. D'Amico, W.P., Clay, W.H., and Mark, A., "Diagnostic Tests for Wick-Type Payloads and High Viscosity Liquids," ARBRL-MR-02913, U.S. Army Ballistic Research Laboratory, Aberdeen Proving Ground, Maryland, April 1979. (AD A072812).
7. D'Amico, W.P., and Clay, W.H., "High Viscosity Liquid Payload Yawsonde Data for Small Launch Yaws," ARBRL-MR-03029, U.S. Army Ballistic Research Laboratory, Aberdeen Proving Ground, Maryland, June 1980. (AD A088411).
8. D'Amico, W.P., Jr., "An Explanation of Spin-Up Instabilities for a 155mm Bindry Projectile," ARBRL-MR-03355, U.S. Army Ballistic Research Laboratory, Aberdeen Proving Ground, Maryland, April 1984. (AD A141534).
9. D'Amico, W. P., Jr., "A Three-Degree-of-Freedom Flight Simulator for Spin-Stabilized Projectiles," AIAA Paper No. 84-0447, AIAA 22ND Aerospace Sciences Meeting, January 1984.
10. Hepner, D. J., "Pressure Measurements in a Liquid-Filled Cylinder Using A Three-Degree of Freedom Flight Simulator," U.S. Army Ballistic Research Laboratory, Aberdeen Proving Ground, Maryland, BRL Report in publication.
11. Hall, P., Sedney, R., and Gerber, N., "Fluid Motion in Spinning, Coning Cylinder via Spatial Eigenfunction Expansions," ARBRL-TR-2813, U.S. Army Ballistic Research Laboratory, Aberdeen Proving Ground, Maryland, August 1987.

REFERENCES (continued)

12. Nusca, Michael J., "Computational Fluid Dynamics Methods for Low Reynolds Number Precessing/Spinning Incompressible Flows," U.S. Army Ballistic Research Laboratory, Aberdeen Proving Ground, Maryland, Memorandum Report in preparation.

# LIST OF SYMBOLS

$a$	Radius of container
$c$	Half height of cylinder
$c/a$	Aspect ratio of container
$\hat{C}_p$	Nondimensional pressure coefficient
$\hat{p}$	Oscillating pressure magnitude
$p$	Spin rate of the container
$Re$	Reynolds number = $a^2 p / \nu$
$r/a$	Radial position/container radius
$\alpha$	Coning angle
$\nu$	Liquid kinematic viscosity
$\rho$	Liquid Density
$\dot{\phi}_1$	Coning rate of the container
$\tau$	Ratio of coning rate to spin rate ( $\dot{\phi}_1/p$ )

# DISTRIBUTION LIST

<u>No. of Copies</u>	<u>Organization</u>	<u>No. of Copies</u>	<u>Organization</u>
12	Administrator Defense Technical Information Center ATTN: DTIC-FDAC Cameron Station, Bldg. 5 Alexandria, VA 22304-6145	4	Commander U.S. Armament RD&E Center US Army AMCCOM ATTN: SMCAR-LCA-F Mr. D. Mertz Mr. A. Loeb SMCAR-LCA-P Mr. F. Scerbo Mr. J. Bera Dover, NJ 07801-5001
1	HQDA DAMA-ART-M Washington, DC 20310	1	Commander US Army Materiel Command ATTN: AMCDRA-ST 5001 Eisenhower Avenue Alexandria, VA 22333-0001
1	Commander US Army ARDEC ATTN: SMCAR-TDC Dover, NJ 07801-5001	1	Commander U.S. AMCCOM ARDEC CCAC Benet Weapons Laboratory ATTN: SMCAR-CCB-TL Watervliet, NY 12189-4050
1	Commander U.S. Armament RD&E Center US Army AMCCOM ATTN: SMCAR-MSI Dover, NJ 07801-5001	1	Commander US Army Aviation Systems Command ATTN: AMSAV-ES 4300 Goodfellow Blvd St. Louis, MO 63120-1798
1	Commander U.S. Armament RD&E Center US Army AMCCOM ATTN: SMCAR-LC Dover, NJ 07801-5001	1	Director US Army Aviation Research and Technology Activity Ames Research Center Moffett Field, CA 94035-1099
1	Commander U.S. Armament RD&E Center US Army AMCCOM ATTN: SMCAR-CAWS-AM Mr. DellaTerga Dover, NJ 07801-5001	1	Commander US Army Communications - Electronics Command ATTN: AMSEL-ED Fort Monmouth, NJ 07703-5000
1	OPM Nuclear ATTN: AMCPM-NUC COL. W. P. Farmer Dover, NJ 07801-5001	1	Commander CECOM R&D Technical Library ATTN: AMSEL-IM-L, (Reports Section) B. 2700 Fort Monmouth, NJ 07703-5000
1	AFWL/SUL Kirtland AFB, NM 87117-6008		

# DISTRIBUTION LIST

<u>No. of Copies</u>	<u>Organization</u>	<u>No. of Copies</u>	<u>Organization</u>
10	C. I. A. OIC/DB/Standard GE47 HQ Washington, DC 20505	1	Director National Aeronautics and Space Administration Langley Research Center ATTN: Tech Library Langley Station Hampton, VA 23365
1	Commandant US Army Infantry School ATTN: ATSH-CD-CS-OR Fort Benning, GA 31905-5400	1	Director US Army Field Artillery Board ATTN: ATZR-BDW Fort Sill, OK 73503
1	Commander US Army Missile Command Research Development and Engineering Center ATTN: AMSMI-RD Redstone Arsenal, AL 35898-5230	1	Commander US Army Dugway Proving Ground ATTN: STEDP-MT Mr. G. C. Travers Dugway, UT 84022
1	Commander US Army Missile Command ATTN: AMSMI-RDK, Mr. R. Deep Redstone Arsenal, AL 35898-5230	1	Commander US Army Yuma Proving Ground ATTN: STEYP-MTW Yuma, AZ 85365-9103
1	Director US Army Missile and Space Intelligence Center ATTN: AIAMS-YDL Redstone Arsenal, AL 35898-5500	2	Director Sandia National Laboratories ATTN: Dr. W. Oberkampff Dr. W. P. Wolfe Division 1636 Albuquerque, NM 87185
1	Commander US Army Tank Automotive Command ATTN: AMSTA-TSL Warren, MI 48397-5000	1	AFATL/DLODL (Tech Info Center) Eglin AFB, FL 32542-5438
1	Director US Army TRADOC Analysis Center ATTN: ATOR-TSL White Sands Missile Range NM 88002-5502	2	Raytheon Company Hartwell Road ATTN: Mr. V.A. Grosso Bedford, MA 01730
1	Commander US Army Development & Employment Agency ATTN: MODE-ORO Fort Lewis, WA 98433-5000	1	Martin-Marietta Corporation ATTN: S.H. Maslen 1450 S. Rolling Road Baltimore, MD 21227
1	Commandant US Army Field Artillery School ATTN: ATSF-GD Fort Sill, OK 73503	1	Carco Electronics 195 Constitution Drive Menlo Park, CA 94025

# DISTRIBUTION LIST

<u>No. of Copies</u>	<u>Organization</u>	<u>No. of Copies</u>	<u>Organization</u>
2	Director Lawrence Livermore National Laboratory ATTN: Mail Code L-35 Mr. T. Morgan Mr. R. Cornell P.O. Box 808 Livermore, CA 94550	1	Illinois Institute of Technology ATTN: Mr. Simon Rosenblat 3300 South Federal Chicago, Illinois 60616
1	University of Wisconsin-Madison Mathematics Research Center ATTN: Dr. John Strikwerda 610 Walnut Street Madison, WI 53706	<u>Aberdeen Proving Ground</u>	
2	Virginia Polytechnic Institute and State University Department of Aerospace Engineering ATTN: Tech Library Dr. Thorwald Herbert Blacksburg, VA 24061	Director, USAMSAA ATTN: AMXSY-D AMXSY-CR, J. O'Brien AMXSY-RA, R. Scungio	
2	University of Southern California Department of Aerospace Engineering ATTN: T. Maxworthy P. Weidman Los Angeles, CA 90007	Commander, USATECOM ATTN: AMSTE-SI-F AMSTE-TE-F, W. Vomocil	
1	University of Virginia Department of Mechanical Aerospace Engineering ATTN: W. E. Scott Charlottesville, VA 22904	PM-SMOKE, Bldg. 324 ATTN: AMCPM-SMK-M	
1	University of Notre Dame Aerospace and Mechanical Engineering Department ATTN: Prof. Thomas J. Mueller South Bend, Indiana 46556	Mr. J. Callahan	
1	Commander David W. Taylor Naval Ship Research and Development Center ATTN: Dr. William K. Blake Bethesda, MD 20084-5000	Cdr, CRDC, AMCCOM ATTN: SMCCR-MU Mr. W. Dee Mr. C. Hughes Mr. F. Dagostin Mr. D. Bromley Mr. C. Jeffers Mr. L. Shaft ATTN: SMCCR-RSP-A Mr. Miles Miller ATTN: SMCCR-SPS-IL SMCCR-RSP-A SMCCR-MU	

# USER EVALUATION SHEET/CHANGE OF ADDRESS

This Laboratory undertakes a continuing effort to improve the quality of the reports it publishes. Your comments/answers to the items/questions below will aid us in our efforts.

1. BRL Report Number \_\_\_\_\_ Date of Report \_\_\_\_\_
2. Date Report Received \_\_\_\_\_
3. Does this report satisfy a need? (Comment on purpose, related project, or other area of interest for which the report will be used.) \_\_\_\_\_  
\_\_\_\_\_  
\_\_\_\_\_
4. How specifically, is the report being used? (Information source, design data, procedure, source of ideas, etc.) \_\_\_\_\_  
\_\_\_\_\_  
\_\_\_\_\_
5. Has the information in this report led to any quantitative savings as far as man-hours or dollars saved, operating costs avoided or efficiencies achieved, etc? If so, please elaborate. \_\_\_\_\_  
\_\_\_\_\_  
\_\_\_\_\_
6. General Comments. What do you think should be changed to improve future reports? (Indicate changes to organization, technical content, format, etc.) \_\_\_\_\_  
\_\_\_\_\_  
\_\_\_\_\_

CURRENT ADDRESS

Name \_\_\_\_\_

Organization \_\_\_\_\_

Address \_\_\_\_\_

City, State, Zip \_\_\_\_\_

7. If indicating a Change of Address or Address Correction, please provide the New or Correct Address in Block 6 above and the Old or Incorrect address below.

OLD ADDRESS

Name \_\_\_\_\_

Organization \_\_\_\_\_

Address \_\_\_\_\_

City, State, Zip \_\_\_\_\_

(Remove this sheet, fold as indicated, staple or tape closed, and mail.)